TABLE 1. Similarity to protein sequences of ORFs in cosmid clone no. 253 derived from *M. intracellulare* serotype 16 strain ATCC 13950^T

ORF	Predicted molecular mass (kDa)	Predicted pI	Exhibits similarity to:	E value	Amino acid identity (no. matched/total no.)	Accession no.
GtfB	45.6	6.35	Glycosyltransferase GtfB	0.0	417/418	BAF45360
Orf 1	45.2	6.10	Putative glycosyltransferase	0.0	416/417	BAF45361
Orf 2	78.9	8.51	Putative acyltransferase	0.0	557/728	BAF45368
Orf 3	31.0	5.88	Putative methyltransferase	2e-89	382/421	NP_218045
Orf 4	15.7	4.94	Conserved hypothetical protein	1e-39	73/129	BAD50406
Orf 5	16.0	4.69	Conserved hypothetical protein	5e-40	75/135	EAX55190
Orf 6	41.1	5.88	Aminotransferase/DegT_DnrJ_EryC1	6e-119	208/357	ABD68440
Orf 7	40.6	9.65	Conserved hypothetical protein	2e-89	178/304	AAS03547
Orf 8	36.7	5.32	Conserved hypothetical protein	2e-52	116/298	CAE06954
Orf 9	22.3	9.79	Putative *N*-acetyltransferase	4e-14	58/166	EAU11841
Orf 10	25.3	7.82	Short-chain dehydrogenase/reductase	7e-47	101/233	EAO61220
Orf 11	23.8	6.05	Putative hydrolase	4e-24	64/196	ABG85599
Orf 12	37.2	6.50	Ketoacyl-acyl carrier protein synthase III	3e-55	126/331	EAX48715
Orf 13	42.5	7.72	Short-chain dehydrogenase/reductase	2e-42	97/248	ZP_01289005
Orf 14	65.8	4.70	Predicted enzyme involved in methoxymalonyl-acyl carrier protein biosynthesis	6e-85	201/575	ABB73590
Orf 15	50.0	6.23	Acyl coenzyme A synthetases	2e-128	233/445	EAT27362
Orf 16	39.1	8.00	Putative glycosyltransferase	2e-106	196/318	NP_855197
Orf 17	37.7	9.46	Putative glycosyltransferase	8e-160	278/323	BAF45369
DrrC	28.6	11.47	Daunorubicin resistance protein C	6e-132	233/261	BAF45370

respectively (Fig. 6; Table S1 in the supplemental material). These results demonstrated unequivocally that the terminal amido-Hex was β configuration and H-2 was in the axial position. The terminal amido-Hex is considered to be derived from glucose or galactose, not Rha.

Next, we explored the genetic mechanism of GPL biosynthesis, because the elongation of carbohydrate chains in serotype-specific GPLs is poorly understood. The *ser2* gene cluster of the *M. avium* serotype 2 strain (31) and a 27.5-kb DNA fragment of the *M. avium* serotype 4 strain (28) were identified to be responsible for the biosynthesis of each OSE in GPLs. Recently, enzymatic characterizations of glycosyltransferase and methyltransferase of nonpolar GPLs have been reported for *Mycobacterium smegmatis* (36, 38). In the serotype-specific polar GPL biosynthesis of MAC, only the *rtfA* gene was functionally clarified to encode the transfer of L-Rha to 6-d-Tal, but which gene cluster transfers the sugars next to L-Rha elongated from 6-d-Tal is unclear.

In this study, we cloned the biosynthetic cluster of the serotype 16 GPL and analyzed its sequence. Seventeen ORFs were detected in the serotype 16 strain, and the sequence homology was analyzed. The transformant of the *M. avium* serotype 1

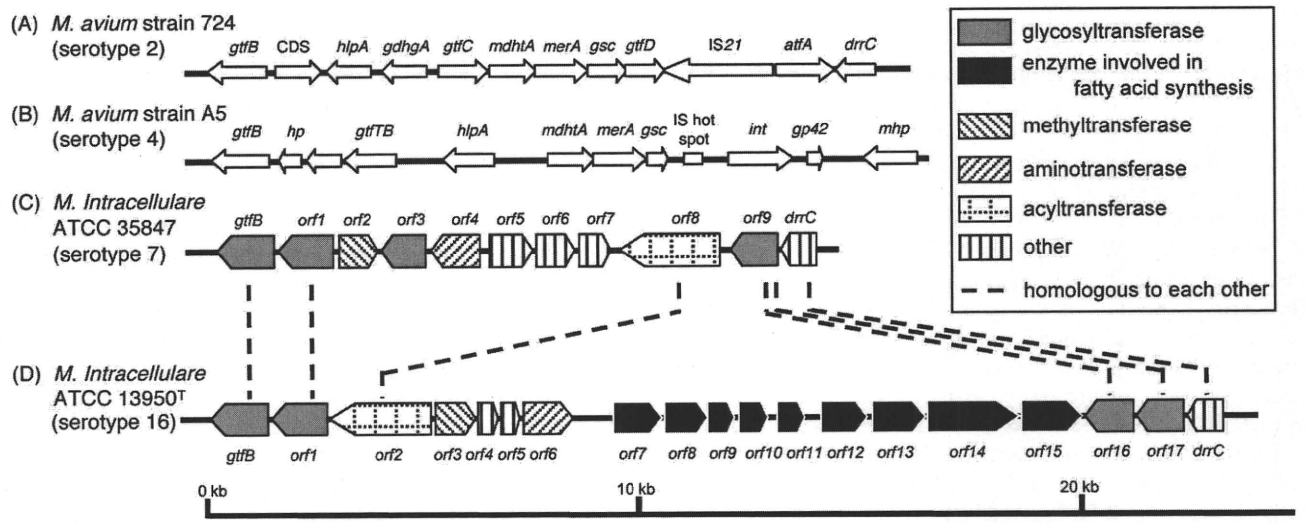

FIG. 7. Comparison and overview of genetic maps of GPL biosynthetic cluster. The *M. avium* strain 724 annotated sequence obtained from GenBank (accession no. AF125999) (A); the *M. avium* strain A5 annotated sequence obtained from GenBank (accession no. AY130970) (B); the *M. intracellulare* ATCC 35847 sequenced in our previous study (GenBank accession no. AB274811) (C); the *M. intracellulare* ATCC 13950^T sequenced in this study (GenBank accession no. AB355138) (D). The orientation of each gene is shown by the direction of the arrow. In panels A and B, putative ORFs not showing homology to known proteins sequences are not depicted. The sequences extending upstream in panels A and B and downstream in panel B are not included in the figure.

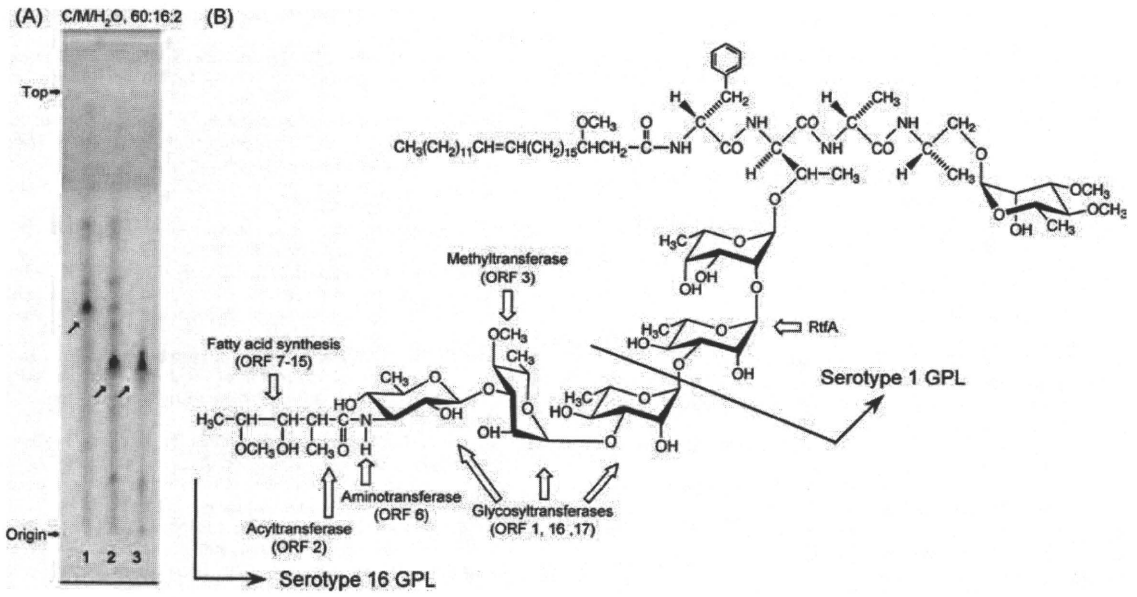

FIG. 8. TLC pattern of *M. avium* serotype 1 and its transformant with cosmid clone no. 253 and proposed complete structure of the serotype 16 GPL. (A) The alkaline-stable lipids derived from *M. avium* serotype 1 (lane 1), its transformant (lane 2), and purified serotype 16 GPL (lane 3) were developed with the solvent system of chloroform-methanol-water (60:16:2, vol/vol/vol). (B) Predicted biosynthesis gene clusters are indicated by arrows.

strain carrying cosmid clone no. 253 produced serotype 16 GPL. These results strongly implied that this *gtfB-drrC* region is responsible for the biosynthesis of the serotype 16-specific GPL. From the structural analysis of the serotype 16 GPL and the sequence of cosmid clone no. 253, it is possible to predict the relationship between the biosynthesis of serotype 16 GPL and the function of each ORF.

The genetic map of the serotype 16 GPL biosynthetic cluster was compared to those of serotype 2 GPL from *M. avium* strain 724, serotype 4 GPL from *M. avium* strain A5, and serotype 7 GPL from *M. intracellulare* strain ATCC 35847^T (12, 18, 28). Significant differences were found in the neighborhood of the conserved region. The genetic organization of the serotype 16 GPL gene cluster was distinct from that of serotype 7, except for some of the ORFs, and the ORFs in this region of serotype 2 and serotype 4 were completely different from ORFs 1 to 17 in serotype 16 (Fig. 7).

In addition to *M. intracellulare* serotype 7 (18) and serotype 16 strains, we have analyzed similar gene clusters of *M. intracellulare* serotype 12 and 17 strains. The sequence homology of the regions of ORF 1 and ORF 17 was highly conserved between only *M. intracellulare* serotype 16 and 17 strains (unpublished data). ORFs 1, 16, and 17 may lead to transfer of the two additional molecules of L-Rha and terminal amido-Hex. ORF 2 was assigned to acyltransferase and may be responsible for biosynthesis of the 3-2′-methyl-3′-hydroxy-4′-methoxy-pentanoyl-amido group in the terminal Hex. ORF 3 is probably responsible for the transfer of the *O*-methyl group at the C-4 position in the third L-Rha from 6-d-Tal. ORF 6 is homologous to aminotransferase and possibly associated with the biosynthesis of an amido group in the terminal Hex. The deduced amino acid sequences of ORF 6 in serotype 16 and ORF 4 in serotype 7 have homologies to DegT_DnrJ_EryC1 aminotransferases. However, these two ORFs are dissimilar to each other. Serotype 16 and 7 GPLs have an amido group at the terminal Hex, although the attachment position is different. The serotype 7 GPL has an amido group at the C-4 position in the terminal Hex, but the serotype 16 GPL has it at the C-3 position. Nine ORFs between ORF 7 and ORF 15 are possibly involved in fatty acid synthesis of the acyl chain moiety linked by an amido bond of the terminal Hex. Taken together, this gene cluster may participate in the biosynthetic pathway of the serotype 16-specific GPL, although further study is needed to clarify the function of each ORF.

Recent studies suggest that GPLs play an important role in the phenotype and pathogenicity of MAC. The colony morphology is considered to be influenced by cell wall GPL. MAC colony phenotypes spontaneously occur from smooth to rough type, and this is due to a mutation lacking GPL (3, 13, 22). The deletion of genomic regions encoding GPL biosynthesis may result in the loss of GPL. Danelishvili et al. demonstrated that the uptake by and growth in macrophages of a MAC mutant with the gene belonging to the GPL synthesis pathway inactivated by transposon insertion were decreased (11). Bhatnagar and Schorey have reported that macrophages infected with MAC release exosomes containing GPLs that result in the transfer of the GPLs to uninfected macrophages and induce a proinflammatory response (4). These findings imply that GPL participates in the pathogenicity of MAC. By contrast, our previous studies have demonstrated that anti-GPL antibodies are detected in the sera of most immunocompetent patients with MAC pulmonary disease and that the detection of anti-GPL antibody is useful for the serodiagnosis of MAC disease (15, 26, 27).

To understand the role of GPLs in MAC and its hosts, it is necessary to define the chemical structure and biosynthesis pathways of GPLs. Elucidation of the structure-function relationship of GPL may open a new avenue for controlling MAC disease.

ACKNOWLEDGMENTS

This work was supported by grants from the Ministry of Education, Culture, Sports, Science, and Technology of Japan, the Japan Health Sciences Foundation, and the Ministry of Health, Labor, and Welfare of Japan (Research on Emerging and Reemerging Infectious Diseases).

We are grateful to Sumihiro Hase (Department of Chemistry, Graduate School of Science, Osaka University, Osaka, Japan) and Hiromi Murakami (Osaka Municipal Technical Research Institute, Osaka, Japan) for helpful discussion.

REFERENCES

1. **Baess, I.** 1983. Deoxyribonucleic acid relationships between different serovars of *Mycobacterium avium*, *Mycobacterium intracellulare* and *Mycobacterium scrofulaceum*. Acta Pathol. Microbiol. Immunol. Scand. **91:**201–203.
2. **Barrow, W. W., T. L. Davis, E. L. Wright, V. Labrousse, M. Bachelet, and N. Rastogi.** 1995. Immunomodulatory spectrum of lipids associated with *Mycobacterium avium* serovar 8. Infect. Immun. **63:**126–133.
3. **Belisle, J. T., K. Klaczkiewicz, P. J. Brennan, W. R. Jacobs, Jr., and J. M. Inamine.** 1993. Rough morphological variants of *Mycobacterium avium*. Characterization of genomic deletions resulting in the loss of glycopeptidolipid expression. J. Biol. Chem. **268:**10517–10523.
4. **Bhatnagar, S., and J. S. Schorey.** 2007. Exosomes released from infected macrophages contain *Mycobacterium avium* glycopeptidolipids and are proinflammatory. J. Biol. Chem. **282:**25779–25789.
5. **Bhatt, A., N. Fujiwara, K. Bhatt, S. S. Gurcha, L. Kremer, B. Chen, J. Chan, S. A. Porcelli, K. Kobayashi, G. S. Besra, and W. R. Jacobs, Jr.** 2007. Deletion of *kasB* in *Mycobacterium tuberculosis* causes loss of acid-fastness and subclinical latent tuberculosis in immunocompetent mice. Proc. Natl. Acad. Sci. USA **104:**5157–5162.
6. **Brennan, P. J., and H. Nikaido.** 1995. The envelope of mycobacteria. Annu. Rev. Biochem. **64:**29–63.
7. **Campo, G. M., S. Campo, A. M. Ferlazzo, R. Vinci, and A. Calatroni.** 2001. Improved high-performance liquid chromatographic method to estimate aminosugars and its application to glycosaminoglycan determination in plasma and serum. J. Chromatogr. B **765:**151–160.
8. **Chatterjee, D., G. O. Aspinall, and P. J. Brennan.** 1987. The presence of novel glucuronic acid-containing, type-specific glycolipid antigens within *Mycobacterium* spp. Revision of earlier structures. J. Biol. Chem. **262:**3528–3533.
9. **Chatterjee, D., and K. H. Khoo.** 2001. The surface glycopeptidolipids of mycobacteria: structures and biological properties. Cell. Mol. Life Sci. **58:** 2018–2042.
10. **Daffe, M., and P. Draper.** 1998. The envelope layers of mycobacteria with reference to their pathogenicity. Adv. Microb. Physiol. **39:**131–203.
11. **Danelishvili, L., M. Wu, B. Stang, M. Harriff, S. Cirillo, J. Cirillo, R. Bildfell, B. Arbogast, and L. E. Bermudez.** 2007. Identification of *Mycobacterium avium* pathogenicity island important for macrophage and amoeba infection. Proc. Natl. Acad. Sci. USA **104:**11038–11043.
12. **Eckstein, T. M., J. T. Belisle, and J. M. Inamine.** 2003. Proposed pathway for the biosynthesis of serovar-specific glycopeptidolipids in *Mycobacterium avium* serovar 2. Microbiology **149:**2797–2807.
13. **Eckstein, T. M., J. M. Inamine, M. L. Lambert, and J. T. Belisle.** 2000. A genetic mechanism for deletion of the *ser2* gene cluster and formation of rough morphological variants of *Mycobacterium avium*. J. Bacteriol. **182:** 6177–6182.
14. **Eckstein, T. M., F. S. Silbaq, D. Chatterjee, N. J. Kelly, P. J. Brennan, and J. T. Belisle.** 1998. Identification and recombinant expression of a *Mycobacterium avium* rhamnosyltransferase gene (*rtfA*) involved in glycopeptidolipid biosynthesis. J. Bacteriol. **180:**5567–5573.
15. **Enomoto, K., S. Oka, N. Fujiwara, T. Okamoto, Y. Okuda, R. Maekura, T. Kuroki, and I. Yano.** 1998. Rapid serodiagnosis of *Mycobacterium avium-intracellulare* complex infection by ELISA with cord factor (trehalose 6, 6′-dimycolate), and serotyping using the glycopeptidolipid antigen. Microbiol. Immunol. **42:**689–696.
16. **Falkinham, J. O., III.** 1996. Epidemiology of infection by nontuberculous mycobacteria. Clin. Microbiol. Rev. **9:**177–215.
17. **Field, S. K., D. Fisher, and R. L. Cowie.** 2004. *Mycobacterium avium* complex pulmonary disease in patients without HIV infection. Chest **126:**566–581.
18. **Fujiwara, N., N. Nakata, S. Maeda, T. Naka, M. Doe, I. Yano, and K. Kobayashi.** 2007. Structural characterization of a specific glycopeptidolipid containing a novel *N*-acyl-deoxy sugar from *Mycobacterium intracellulare* serotype 7 and genetic analysis of its glycosylation pathway. J. Bacteriol. **189:**1099–1108.
19. **Gerwig, G. J., J. P. Kamerling, and J. F. G. Vliegenthart.** 1978. Determination of the D and L configuration of neutral monosaccharides by high-resolution capillary G.L.C. Carbohydr. Res. **62:**349–357.
20. **Hakomori, S.** 1964. A rapid permethylation of glycolipid, and polysaccharide catalyzed by methylsulfinyl carbanion in dimethyl sulfoxide. J. Biochem. (Tokyo) **55:**205–208.
21. **Heidelberg, T., and O. R. Martin.** 2004. Synthesis of the glycopeptidolipid of *Mycobacterium avium* serovar 4: first example of a fully synthetic C-mycoside GPL. J. Org. Chem. **69:**2290–2301.
22. **Howard, S. T., E. Rhoades, J. Recht, X. Pang, A. Alsup, R. Kolter, C. R. Lyons, and T. F. Byrd.** 2006. Spontaneous reversion of *Mycobacterium abscessus* from a smooth to a rough morphotype is associated with reduced expression of glycopeptidolipid and reacquisition of an invasive phenotype. Microbiology **152:**1581–1590.
23. **Kaufmann, S. H.** 2001. How can immunology contribute to the control of tuberculosis? Nat. Rev. Immunol. **1:**20–30.
24. **Khoo, K. H., D. Chatterjee, A. Dell, H. R. Morris, P. J. Brennan, and P. Draper.** 1996. Novel *O*-methylated terminal glucuronic acid characterizes the polar glycopeptidolipids of *Mycobacterium habana* strain TMC 5135. J. Biol. Chem. **271:**12333–12342.
25. **Khoo, K. H., E. Jarboe, A. Barker, J. Torrelles, C. W. Kuo, and D. Chatterjee.** 1999. Altered expression profile of the surface glycopeptidolipids in drug-resistant clinical isolates of *Mycobacterium avium* complex. J. Biol. Chem. **274:**9778–9785.
26. **Kitada, S., R. Maekura, N. Toyoshima, N. Fujiwara, I. Yano, T. Ogura, M. Ito, and K. Kobayashi.** 2002. Serodiagnosis of pulmonary disease due to *Mycobacterium avium* complex with an enzyme immunoassay that uses a mixture of glycopeptidolipid antigens. Clin. Infect. Dis. **35:**1328–1335.
27. **Kitada, S., Y. Nishiuchi, T. Hiraga, N. Naka, H. Hashimoto, K. Yoshimura, K. Miki, M. Miki, M. Motone, T. Fujikawa, K. Kobayashi, I. Yano, and R. Maekura.** 2007. Serological test and chest computed tomography findings in patients with *Mycobacterium avium* complex lung disease. Eur. Respir. J. **29:**1217–1223.
28. **Krzywinska, E., and J. S. Schorey.** 2003. Characterization of genetic differences between *Mycobacterium avium* subsp. avium strains of diverse virulence with a focus on the glycopeptidolipid biosynthesis cluster. Vet. Microbiol. **91:**249–264.
29. **Maekura, R., Y. Okuda, A. Hirotani, S. Kitada, T. Hiraga, K. Yoshimura, I. Yano, K. Kobayashi, and M. Ito.** 2005. Clinical and prognostic importance of serotyping *Mycobacterium avium-Mycobacterium intracellulare* complex isolates in human immunodeficiency virus-negative patients. J. Clin. Microbiol. **43:**3150–3158.
30. **Marras, T. K., and C. L. Daley.** 2002. Epidemiology of human pulmonary infection with nontuberculous mycobacteria. Clin. Chest Med. **23:**553–567.
31. **Maslow, J. N., V. R. Irani, S. H. Lee, T. M. Eckstein, J. M. Inamine, and J. T. Belisle.** 2003. Biosynthetic specificity of the rhamnosyltransferase gene of *Mycobacterium avium* serovar 2 as determined by allelic exchange mutagenesis. Microbiology **149:**3193–3202.
32. **McClatchy, J. K.** 1981. The seroagglutination test in the study of nontuberculous mycobacteria. Rev. Infect. Dis. **3:**867–870.
33. **McCloskey, J. A.** 1969. Mass spectrometry, p. 402. *In* J. M. Lowenstein (ed.), Methods in enzymology: lipid, vol. 14. Academic Press, New York, NY.
34. **McNeil, M., H. Gaylord, and P. J. Brennan.** 1988. *N*-formylkansosaminyl-(1-3)-2-*O*-methyl-D-rhamnopyranose: the type-specific determinant of serovariant 14 of the *Mycobacterium avium* complex. Carbohydr. Res. **177:**185–198.
35. **McNeil, M., A. Y. Tsang, and P. J. Brennan.** 1987. Structure and antigenicity of the specific oligosaccharide hapten from the glycopeptidolipid antigen of *Mycobacterium avium* serotype 4, the dominant *Mycobacterium* isolated from patients with acquired immune deficiency syndrome. J. Biol. Chem. **262:** 2630–2635.
36. **Miyamoto, Y., T. Mukai, N. Nakata, Y. Maeda, M. Kai, T. Naka, I. Yano, and M. Makino.** 2006. Identification and characterization of the genes involved in glycosylation pathways of mycobacterial glycopeptidolipid biosynthesis. J. Bacteriol. **188:**86–95.
37. **Odham, G., and E. Stenhagen.** 1972. Fatty acids, p. 211–228. *In* G. R. Waller (ed.), Biochemical application of mass spectrometry. Wiley-Interscience, New York, NY.
38. **Patterson, J. H., M. J. McConville, R. E. Haites, R. L. Coppel, and H. Billman-Jacobe.** 2000. Identification of a methyltransferase from *Mycobacterium smegmatis* involved in glycopeptidolipid synthesis. J. Biol. Chem. **275:**24900–24906.
39. **Supply, P., E. Mazars, S. Lesjean, V. Vincent, B. Gicquel, and C. Locht.** 2000. Variable human minisatellite-like regions in the *Mycobacterium tuberculosis* genome. Mol. Microbiol. **36:**762–771.
40. **Tsang, A. Y., J. C. Denner, P. J. Brennan, and J. K. McClatchy.** 1992. Clinical and epidemiological importance of typing of *Mycobacterium avium* complex isolates. J. Clin. Microbiol. **30:**479–484.
41. **Wayne, L. G., and H. A. Sramek.** 1992. Agents of newly recognized or infrequently encountered mycobacterial diseases. Clin. Microbiol. Rev. **5:**1–25.
42. **Woods, A., and J. R. Couchman.** 2001. Proteoglycan isolation and analysis, p. 10.7.1–10.7.19. *In* J. S. Bonifacino, M. Dasso, J. B. Harford, J. Lippincott-Schwartz, and K. M. Yamada (ed.), Current protocols in cell biology. Wiley Interscience, Hoboken, NJ.

International Immunology, Vol. 20, No. 7, pp. 849–860
doi:10.1093/intimm/dxn043

Human T_h1 differentiation induced by lipoarabinomannan/lipomannan from *Mycobacterium bovis* BCG Tokyo-172

Toshihiro Ito[1], Akihiro Hasegawa[1], Hiroyuki Hosokawa[1], Masakatsu Yamashita[1], Shinichiro Motohashi[1], Takashi Naka[2], Yuko Okamoto[2], Yukiko Fujita[2], Yasuyuki Ishii[3], Masaru Taniguchi[3], Ikuya Yano[2], and **Toshinori Nakayama[1]**

[1]Department of Immunology, Graduate School of Medicine, Chiba University, 1-8-1 Inohana, Chuo-ku, Chiba 260-8670, Japan
[2]Japan BCG Laboratory, 3-1-5 Matsuyama, Kiyose, Tokyo 204-0022, Japan
[3]RIKEN Research Center for Allergy and Immunology, 1-7-22 Suehiro-cho, Tsurumi-ku, Yokohama, Kanagawa 230-0045, Japan

Keywords: DC, T_h1/T_h2, vaccination

Abstract

Mycobacterium tuberculosis **(tubercle bacilli) and the related acid-fast bacteria including *Mycobacterium bovis* Bacille Calmett–Guerin (BCG) have a characteristic cell wall (CW) containing various lipoglycans and glycolipids. Such lipoglycans have been reported to activate type-I inflammatory responses via dendritic cells (DCs) through Toll-like receptor 2. In this study, lipoglycans, lipoarabinomannan (LAM), lipomannan (LM) and phosphatidylinositol mannoside (PIM), were purified from the CW fractions of *M. bovis* BCG Tokyo-172, and the effect on the differentiation of human peripheral blood naive CD4 T cells into T_h1 and T_h2 was examined. LAM/LM molecules enhanced T_h1 differentiation under both T_h1 and T_h2 conditions, whereas some other glycolipids and phospholipid enhanced T_h2 differentiation under T_h2 conditions. Other components had little effect under the given conditions. Even in highly purified CD4 T cell cultures, LAM/LM enhanced T_h1 generation only under T_h1 culture conditions. These results indicate that LAM/LM possesses a potent augmenting activity in T_h1 differentiation in human CD4 T cells. LAM/LM appeared to act directly on naive CD4 T cells to enhance T_h1 differentiation under T_h1 culture conditions, while acting indirectly to up-regulate the generation of T_h1 cells via IL-12/DCs under T_h1 and T_h2 conditions. Therefore, these results provide the first evidence indicating that LAM/LM from *M. bovis* BCG may possess a potent modulating activity in the human system, and thus supporting the strategy for the use of BCG components in the vaccine development for such T_h2 diseases as allergic asthma and rhinitis.**

Introduction

The mycobacterial cell envelope consists of diverse lipophylic components such as mycoloyl glycolipids, lipomannan (LM)/lipoarabinomannans (LAM), lipopeptides and phosphatidylinositol mannosides (PIMs) or cardiolipin as shown schematically in Fig. 1 (1, 2). LAM is a major amphipathic molecule in the cell wall (CW) components of mycobacteria and is regarded as a modulin acting through its diverse immunoregulatory and anti-inflammatory effects, which may support the survival of the mycobacteria within the infected hosts. These effects are mediated by the inhibition of IFN-γ-dependent activation of macrophages (3, 4), inhibition of antigen-induced T cell proliferation (5) and scavenging of oxygen-derived free radicals (6). LAM acts as a virulence factor responsible for macrophage deactivation by mannose receptor down-regulation and also is implicated in phagocytosis of mycobacteria (7). Furthermore, PIMs, that are assumed to be precursors of LM and LAM have recently been proposed to recruit NKT cells, which play a primary role in the granulomatous response in mycobacterial infection (8, 9). The precursor–product relationship of phosphatidylinositol (PI), PIMs, LM and LAM has recently been proposed based on biosynthetic (1, 10) and genetic studies (11, 12), but the details of this pathway remain unclear. On the other hand, however, the structures of LAM from many species of mycobacteria, nocardia and rhodococcus including *Mycobacterium tuberculosis*, *Mycobacterium leprae*, *M. bovis* Bacille Calmett–Guerin (BCG) and *Mycobacterium smegmatis* have been vigorously investigated over the last

Correspondence to: T. Nakayama; E-mail: tnakayama@faculty.chiba-u.jp

Transmitting editor: A. Singer

Received 8 November 2007, *accepted* 8 April 2008

Advance Access publication 9 May 2008

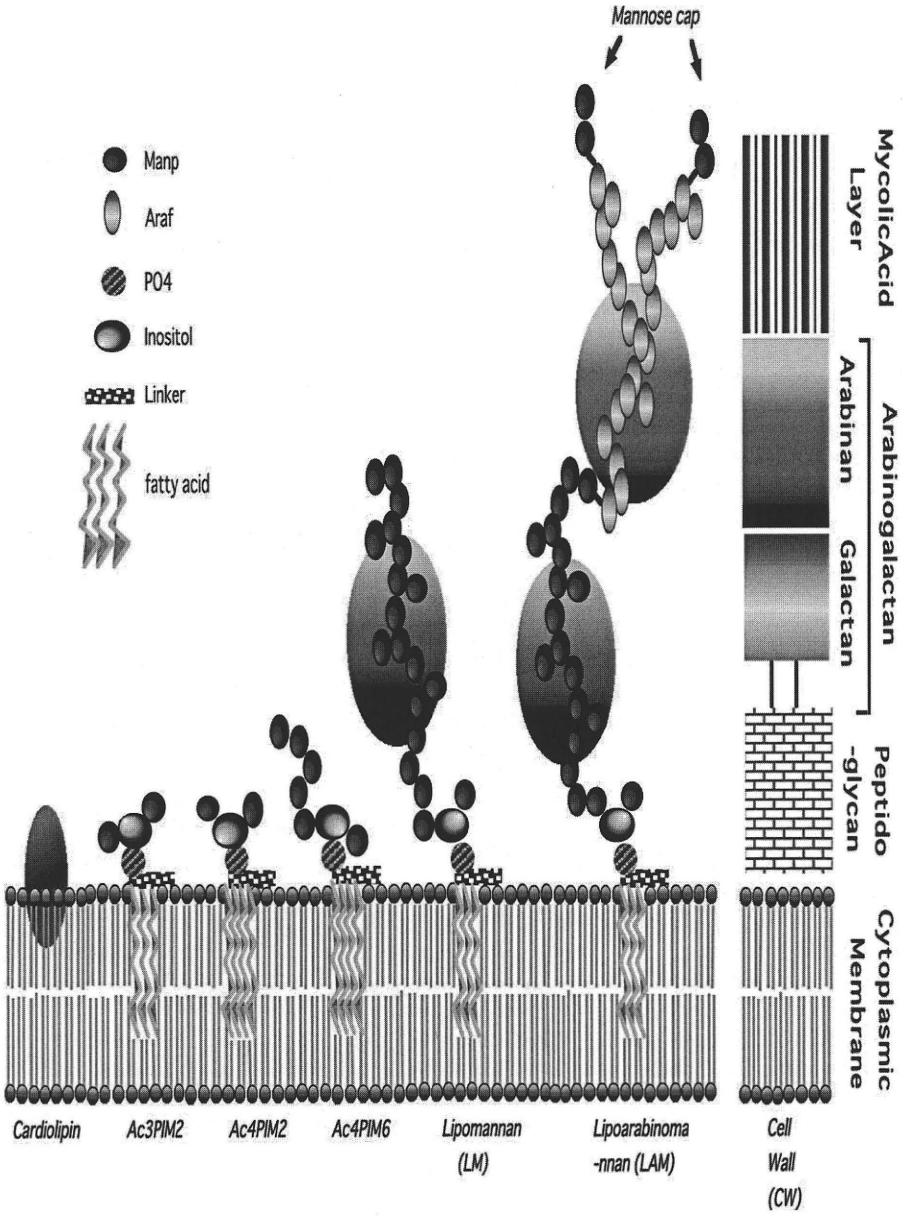

Fig. 1. Schematic structure of the mycobacterial cell envelopes. The individual compartment was shown to be a cytoplasmic membrane, peptidoglycan layer, arabinogalactan and mycolic acid layer (right side). The structures of the major lipid and lipoglycan molecules from BCG Tokyo-172 are shown; cardiolipin, Ac3PIM2, Ac4PIM2, Ac4PIM6, LM and LAM.

decade. LAM is a complex lipoglycan composed of D-mannan and D-arabinan attached to a PI moiety that anchors to the cytoplasmic membrane in the mycobacterial cell envelope (13). Although fatty acyl moiety is consistent among mycobacteria, the carbohydrate chain structure of LAM differs greatly according to the mycobacterial species, such as LAM with mannose caps (ManLAM), AraLAM and PILAM. However, the relationship between the molecular structure and immunomodulating activity of LAM has not yet been fully established especially in human immunocompetent systems.

Dendritic cells (DCs) play a crucial role in the induction of cellular immunity against intracellular pathogens including mycobacteria (14–16). Human or murine myeloid DC infected with *M. tuberculosis* or *M. bovis* BCG induced the maturation with an increased IL-12 production (17, 18) and induced a potent anti-tuberculous immunity against experimental tuberculosis in mice (19). A T_h1 cytokine IFN-γ has been identified as a key cytokine controlling mycobacterial infections (20–23). Patients defective in genes for IFN-γ or the IFN-γR are prone to serious mycobacterial infections (24). Therefore, IFN-γ plays a crucial role in anti-mycobacterial immunity. ManLAM, which is produced by slow-growing mycobacteria including *M. bovis* BCG, which has been reported to exert an immunosuppressive effect (25–27) and contributes to the persistence of slow-growing mycobacteria in humans. In contrast, LAM having phospho-myo-inositol units and LAM without capping are called PILAM and are produced from fast-growing mycobacteria. PILAM produces

a variety of pro-inflammatory cytokines through the activation of Toll-like receptor 2 (TLR2) (28–30). LM was shown to activate the macrophages in a TLR2-dependent and TLR4- and TLR6-independent manner (31–33). The balance of ManLAM/LM could thus be a parameter influencing the net immune responses against mycobacteria (34). Many investigators have reported that LAM/LM molecules induced type-I responses accompanied with the enhanced production of inflammatory cytokines, such as tumor necrosis factor α (TNFα) and IL-12 in DCs, and increased CD1 molecules on antigen-presenting cells (APCs). However, the regulation of the T_h1/T_h2 balance in the human immune system with PBMC induced by LAM/LM has not yet been reported.

In the present study, purified ManLAM/LM molecules from *M. bovis* BCG Tokyo-172 were structurally and functionally characterized, and the effect of LAM/LM on T_h1/T_h2 differentiation was assessed using an established human T_h1/T_h2 differentiation culture system. As a result, two distinct regulatory pathways were identified in which mycobacterial LAM/LM controls the balance of T_h1/T_h2 directly or indirectly via APCs.

Methods

Bacterial strain and growth conditions

Mycobacterium bovis BCG Tokyo-172 (ATCC 35737) was grown as a surface culture at 37°C in Sauton medium for 8 days. The bacterial culture was harvested by centrifugation after autoclaving at 121°C for 15 min.

Isolation and purification of LAM/LM, phosphatidylinositol dimannoside, hexamannoside and cardiolipin

Lipids were extracted with chloroform–methanol (2:1, by volume) and the crude lipids were separated by the solvent fractionation method (35). The PIMs [phosphatidylinositol dimannoside (PIM2) and hexamannoside (PIM6)] and cardiolipin were isolated from the chloroform-soluble fraction by thin-layer chromatography on a silica gel (Uniplate and Analtech) with the solvent system of chloroform–methanol–water (65:25:4, by volume). For purification of LAM/LM, the cells were re-suspended in deionized water and were passed three times through a French pressure cell (5501-MF, OHTAKE WORKS, Tokyo, Japan) at a pressure of 180 Mpa and disrupted. The unbroken cells were removed by centrifugation twice at 6760 × *g* for 20 min at 25°C. The broken cells (crude CW fraction) were separated from the supernatant by ultracentrifugation at 18 000 × *g* for 1 h at 25°C, and the supernatant containing lipoglycan was lyophilized. Contaminating glucans, proteins, DNA and RNA were removed by enzymatic degradation using α-amylase, trypsin, DNase 1 and RNase treatments followed by dialysis. An equal volume of 90% phenol was then added to the water containing lipoglycans, and the mixture was incubated with shaking at 68°C for 1 h. After separation of the aqueous phase from the phenol layer by low-speed centrifugation, the phenolic phase was again extracted with an equal volume of water. The two aqueous extracts were combined and residual phenol was removed by extraction with the chloroform. The aqueous phase containing the crude lipoglycans was evaporated to dryness. The crude lipoglycans were subjected to Triton X-114 phase separation (36). The resulting lipoglycans (LAM/LM) were re-suspended in buffer A, 0.2 M NaCl, 0.25% sodium deoxycholate (w/v), 1 mM EDTA and 10 mM Tris, pH 8.0, and loaded onto gel filtration columns (Superdex 75 prep grade column, 50 × 1 cm, Amersham Bioscience) and eluted with buffer A at a flow rate 0.2 ml min^{-1}. The fractions were collected and analyzed by SDS–PAGE followed by silver staining. The LAM and LM fractions pooled were dialyzed extensively against water, lyophilized and stored at −20°C.

Mass spectrometric analysis of lipoglycans LAM and LM

MALDI TOF-MS spectra were acquired on a Voyager DE-STR MALIDI TOF-MS spectrometer (Applied Biosystem) with a pulse laser emitting at 337 nm. The samples were analyzed in the reflectron mode with an accelerating voltage operating in the negative ion mode of 25 kV. As the matrix, 2,5-dihydroxybenzoic acid was used at a concentration of 10 mg ml^{-1}, in a mixture of water. A total of 1.0 μl of lipoglycan, at a concentration of 10 mg ml^{-1}, was mixed with 1.0 μl of the matrix solution. The sample mixture was applied onto the sample plate as a 1.0-μl droplet. The samples were then allowed to crystallize at room temperature.

Preparation of human PBMCs and CD4 T cells

Whole blood was obtained from six healthy donor volunteers between 24 and 50 years old. The protocol was approved by the Institutional Ethics Committee (No. 1972). PBMCs were isolated by Ficol-Paque (Pharmacia-Upjohn, Uppsala, Sweden) gradient centrifugation (37). Naive $CD4^+$ T cells were stained with anti-CD8/CD45RO–FITC and then purified using anti-FITC magnetic beads (Miltenyi Biotec) and AutoMACS cell sorter (Miltenyi Biotec) by negative sorting.

Preparation of highly purified naive CD4 T cells and monocyte derived dendritic cells

Highly purified naive CD4 T cells ($CD4^+$, $CD45RA^+$) were prepared using a human naive CD4 T cell isolation kit (Miltenyi Biotec Inc.) and an AutoMACS sorter. The purity ($CD4^+$, $CD45RA^+$) was >95%. For preparation of monocyte derived dendritic cells, whole PBMCs were allowed to adhere to culture flasks for 1.5–2 h at 37°C and then adherent cells were cultured for 5–7 days in the presence of human IL-4 (500 U ml^{-1}, R&D Systems, Minneapolis, MN, USA) and human granulocyte macrophage colony-stimulating factor (800 U ml^{-1}) (38). $CD11c^+$ cells were purified using a MACS separation column (Miltenyi Biotec) according to the manufacturer's protocol. Purified DCs (7.5 × 10^5 per well) were added to the *in vitro* T cell differentiation culture.

In vitro *T cell differentiation culture*

Naive CD4 T cells or highly purified naive CD4 T cells (7.5 × 10^5 per well) were stimulated with 20 μg ml^{-1} immobilized anti-CD3 mAb (Raritan, Somerset County, NJ, USA) for 2 days in the presence of 50 U ml IL-2 (Shionogi & Co., Ltd, Osaka, Japan), 1 ng ml^{-1} IL-12 (R&D Systems) and 5 μg ml^{-1} anti-IL-4 mAb (BD Bioscience) under T_h1 culture conditions (39). For T_h2 conditions, the cells were stimulated with 20 μg ml^{-1} immobilized anti-CD3 mAb in the presence of

50 U ml^{-1} IL-2, 1 ng ml^{-1} IL-4 (R&D Systems) and 5 μg ml^{-1} anti-IFN-γ mAb (BD Bioscience). For neutral conditions, the cells were stimulated with 20 μg ml^{-1} immobilized anti-CD3 mAb in the presence of 50 U ml^{-1} IL-2. The cells were then transferred to new plates and cultured for another 5 days in the presence of cytokines and antibodies used in the same culture conditions. Since IL-4-producing cells were not induced significantly in a week culture under T_h2 culture conditions, two cycles of the stimulation were used. Where indicated, anti-IL-12 mAb (2 μg ml^{-1}, U-CyTech Biosciences, Utrecht, The Netherlands) was added to the culture. The final concentration of CW, LAM/LM, PIM2 and PIM6 was adjusted to 100 μg ml^{-1}.

Intracellular staining of IL-4 and IFN-γ and flow cytometry analysis

The cultured T cells were re-stimulated with PMA (10 ng ml^{-1}) and ionomycin (1 μM) for 4 h in the presence of 2 μM monensin, which inhibited the secretion of newly produced protein. Next, the cells were fixed with 4% PFA for 10 min at room temperature and were permeabilized with 0.5% Triton X-100 (in 50 mM NaCl, 5 mM EDTA and 0.02% NaN_3, pH7.5) for 10 min on ice. After blocking with 3% BSA in PBS for 15 min, the cells were incubated on ice for 45 min with anti-IFN-γ–FITC, IL-4–PE (BD Bioscience) and CD4–allophycocyanin (BD Bioscience) as described (39). A flow cytometry analysis was performed on FACScalibur® (Becton Dickinson, Franklin Lakes, NJ, USA), and the results were analyzed using the CELLQUEST® software program (Becton Dickinson).

Results

Purification of LAM/LM from BCG Tokyo-172

The experimental procedures to extract LM and LAM from *M. bovis* BCG Tokyo-172 are based on successive detergent and phenolic extractions, thus leading to the recovery of nucleic acid-, protein- and lipid-free materials.

LAM and LM fractions were fully separated and collected by gel filtration chromatography (Fig. 2A). The purity of each component was assessed by SDS–PAGE (Fig. 2B), and the molar ratios of mannose and arabinose in LAM and LM fractions were analyzed by gas chromatography/mass spectrometry (data not shown) and MALDI TOF-MS spectrometry (Fig. 2C and D). The accurate molecular weights of LAM and LM were determined on the basis of the deprotonated ions $[M-H]^-$. As a result, LAMs from *M. bovis* BCG TOKYO-172 was identified to be highly heterogeneous lipoglycans possessing 16–46 mannose residues and 50–60 arabinoses and three acyl groups with the molecular weight ranging from 11 000 to 19 000 Da (Fig. 2C). On the other hand, LM from *M. bovis* BCG Tokyo-172 showed clear $[M-H]^-$ ions in MALDI TOF-MS analysis ranging from m/z 3600 to 8400,

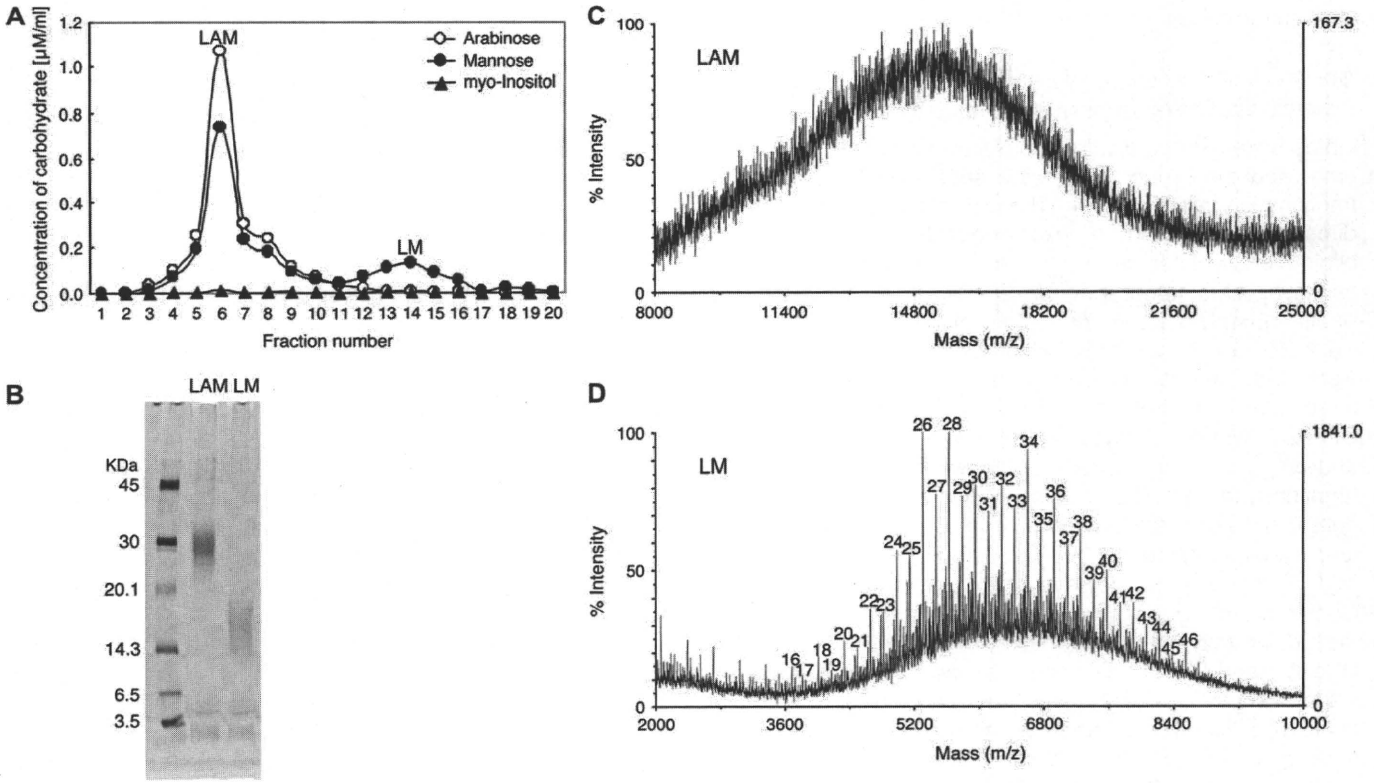

Fig. 2. Purification of BCG Tokyo-172 LAM and LM and MALDI TOF-MS spectra of the purified fractions. (A) Gel filtration profile of the Triton X-114 fraction containing lipoglycans. The fraction was loaded onto a Superdex 75 prep grade column and eluted with deoxycholate buffer. (B) SDS–PAGE analysis of purified fractions from LAM and LM. (C) Negative ion mode MALDI TOF-MS spectra of the fraction LAM. (D) Negative MALDI TOF-MS spectra of the fraction LM that corresponded to triacylated forms, with 2C16 and 1C19 fatty acids. The numbers shown in the figure represent the number of mannose residues in LM.

indicating that they have 16–48 mannoses and three acyl groups, C16:0, C16:0 and C19:0, mainly (Fig. 2D).

Effects of LAM/LM in human T_h1/T_h2 cell differentiation

An *in vitro* T_h1/T_h2 differentiation culture system was used with human peripheral blood naive CD4 T cells to evaluate the effects of BCG CW components on human T_h1/T_h2 differentiation. First, the effect of whole CW fraction and the mixture of LAM/LM were assessed. BCG CW components were homogenously suspended in PBS and then the vehicle was used as negative control. Under T_h1 culture conditions, the generation of T_h1 cells (IFN-γ positive and IL-4 negative) was significantly enhanced in the presence of CW and LAM/LM (37.5 versus 80.7 and 73.6%, respectively) in comparison to the vehicle control (Fig. 3A). Under T_h2 culture conditions, the generation of T_h2 (IL-4 positive and IFN-γ negative) was inhibited significantly in the presence of CW and LAM/LM (25.7 versus 12.5 and 13.9%, respectively), whereas that of T_h1 was enhanced greatly (10.9 versus 37.6 and 38.8%, respectively). Under neutral conditions, they were cultured for 1 week (Fig. 3A) or 2 weeks (Fig. 3B) with anti-CD3 mAb with IL-2, and the generation of IFN-γ-producing T_h1 and that of IL-4-producing T_h2 were marginal, and the levels of these T_h1/T_h2 were not affected in the presence of CW or LAM/LN. These results indicate that CW and LAM/LM enhance T_h1 differentiation and inhibit T_h2 differentiation under both T_h1 and T_h2 culture conditions. Ac4PIM2, Ac3PIM2, Ac4PIM6 and cardiolipin, which are precursors of LAM/LM and cytoplasmic membrane lipids, did not enhance T_h1 differentiation significantly, but showed some induction of T_h2 under T_h2 culture conditions (Fig. 3C), indicating that the precursors of LAM/LM may have different effects from LAM/LM on T_h1/T_h2 differentiation in human PBMC cultures *in vitro* under the given conditions.

Next, to confirm the effects of CW and LAM/LM on T_h1/T_h2 differentiation, the analysis was extended to naive CD4 T cells from 10 healthy volunteers. Similar T_h1/T_h2 cultures were used in the presence of CW and LAM/LM (Fig. 4). As expected, the addition of CW and LAM/LM to the induction culture enhanced T_h1 differentiation under both T_h1 (Fig. 4A and C) and T_h2 culture conditions (Fig. 4B and D, right panels), and the addition of CW suppressed T_h2 differentiation under T_h2 culture conditions (Fig. 4B, left panel) in most of the healthy volunteers tested. The addition of LAM/LM inhibited T_h2 differentiation in some but not all individuals (Fig. 4D, left panel). Thus, these results clearly indicate that CW and LAM/LM enhance T_h1 differentiation while they inhibit T_h2 differentiation. No significant effect was observed under neutral conditions (Supplementary Figure 1, available at *International Immunology* Online). Ac4PIM2, Ac3PIM2, Ac4PIM6 and cardiolipin did not affect the levels of either T_h1 differentiation under both T_h1 and T_h2 culture conditions

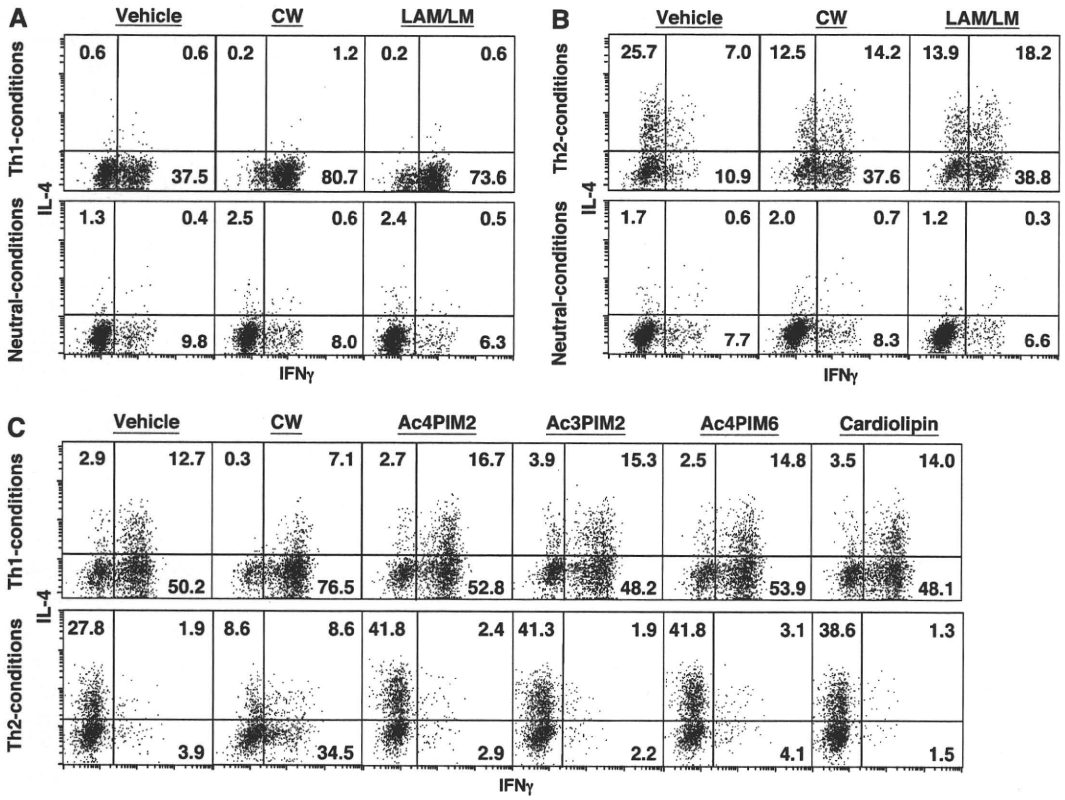

Fig. 3. Effect of BCG CW components on human T_h1/T_h2 differentiation. Naive CD4 T cells from human PBMC were stimulated with anti-CD3 (20 μg ml^{-1}) in the presence of anti-IFN-γ mAb, IL-4 and IL-2 (T_h2 conditions), in the presence of anti-IL-4 mAb, IL-12 and IL-2 (T_h1 conditions) or in the presence of IL-2 (neutral conditions). The cultured cells were subjected to intracellular staining with anti-IL-4 and anti-IFN-γ. A 1-week culture (A) and a 2-week culture (B) were performed. CW and LAM/LM (100 μg ml^{-1}) (A and B) or Ac4PIM2, Ac3PIM2, Ac4PIM6 or cardiolipin (C) (100 μg ml^{-1}) were added to the culture.

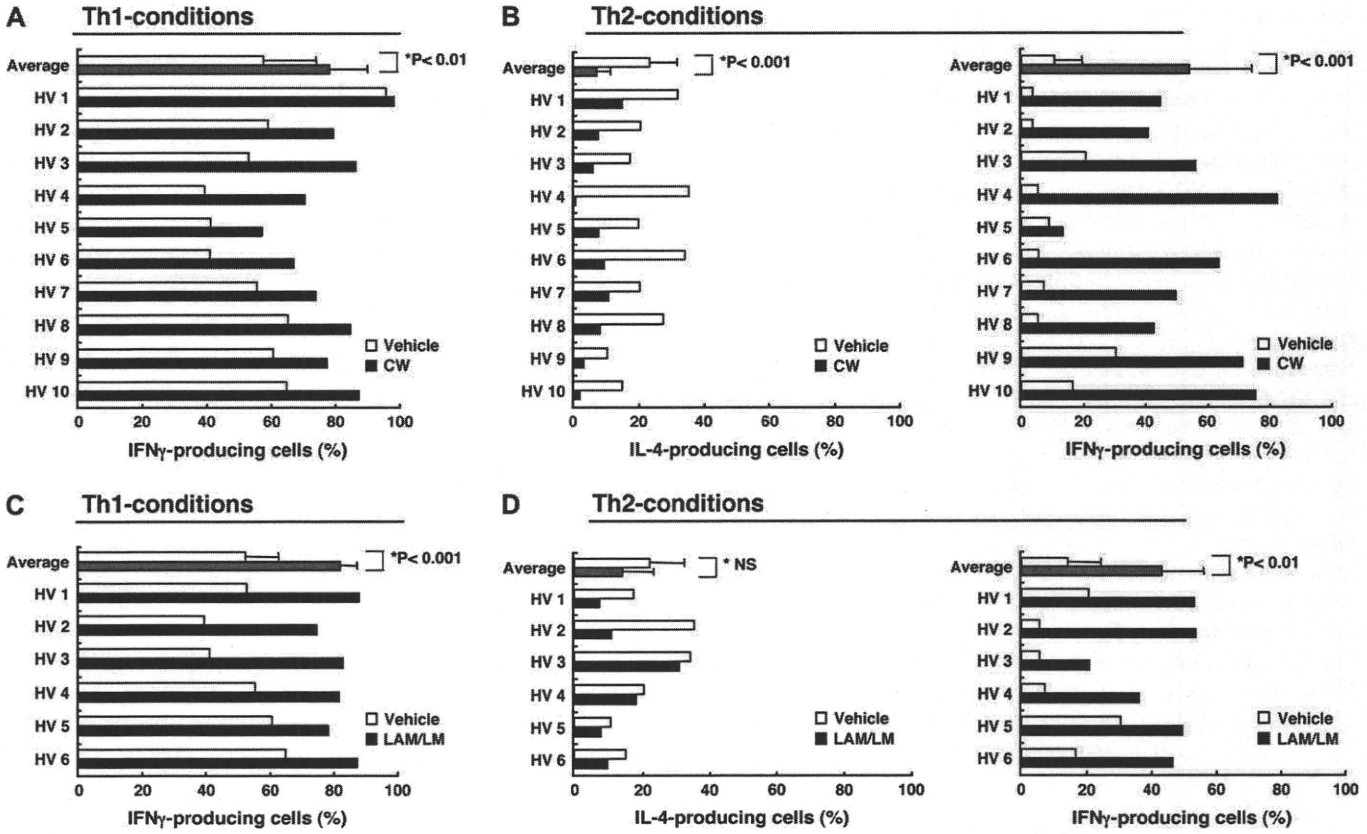

Fig. 4. Effect of BCG CW and LAM/LM on T_h1/T_h2 differentiation using ten human healthy donor PBMCs. T_h1/T_h2 cell differentiation cultures with naive CD4 T cells from 10 human PBMCs were performed as described in Fig. 3. CW (A and B) and LAM/LM (C and D) (100 μg ml^{-1}) were added. The mean values with standard deviations are also shown. Statistical analysis was done using Student's *t*-test.

(Fig. 5A–H). In addition, the effect of these components on the differentiation of T_h2 was seen in some cultures but the effects were marginal (Fig. 5B, D, F and H).

Cellular mechanisms underlying the LAM/LM-mediated modulation of human T_h1/T_h2 differentiation

The CD4 T cells from human PBMC, which were used in the experiments described above, were prepared by removing $CD8^+CD45RO^+$ cells with an AutoMACS cell sorter as described in Methods. These cell preparations contain substantial numbers of forward-$scatter^{high}$/side-$scatter^{high}$ cells and CD4-negative cells (Fig. 6A, Fraction A). To further enrich CD4 T cells, a naive CD4 T cell isolation kit and AutoMACS cell sorter were used (Fig. 6B, Fr. B). Positive cells for CD8, CD14, CD16, CD19, CD36, CD45RO, CD56, CD123, TCRγδ or glycophorin were removed in this separation procedure. Concurrently, CD11c-positive *in vitro* generated DCs from PBMCs were isolated using PE-conjugated anti-CD11c mAb, anti-PE magnetic beads and AutoMACS (Fig. 6C, Fr. C). Using these crude naive CD4 T cells (Fr. A), highly purified naive CD4 T cells (Fr. B) and the mixture of purified naive CD4 T cells (Fr. B) and enriched DCs (Fr. C), T_h1/T_h2 differentiation cultures were set in the presence of LAM/LM (Fig. 7). Under T_h1 culture conditions, the generation of IFN-γ-producing cells was enhanced by LAM/LM in all cultures with Fr. A, Fr. B and the mixture of Fr. B and Fr. C (Fig. 7A, left). Under neutral conditions, the induction of IFN-γ-producing cells was marginal after a 1-week culture with Fr. A and Fr. B, and no significant effect was observed (Fig. 7A, right). However, in the culture of the mixture of purified naive CD4 T cells (Fr. B) and DCs (Fr. C), the generation of IFN-γ-producing cells was enhanced. Under T_h2 culture conditions, the enhancement of the generation of IFN-γ-producing cells and the inhibition of the generation of IL-4-producing cells in the presence of LAM/LM were observed in the cultures with Fr. A but not in the cultures with Fr. B (Fig. 7B, left panels). Interestingly, however, the effects of LAM/LM were restored by the addition of DCs (Fr. C) into purified naive CD4 T cells (Fr. B) (Fig. 7B, left bottom). The addition of anti-IL-12 mAb inhibited the enhancement of the generation of IFN-γ-producing cells (10.3 versus 3.2%) and the suppression of the generation of IL-4-producing cells (24.4 versus 40.3%) in the Fr. A cultures. No effect was observed in the Fr. B cultures (15.8 versus 15.4%). A small but moderate rescue effect was observed in the culture with the mixture of Fr. B and Fr. C (3.1 versus 4.5%). Basically, the same pattern as that seen after the 1-week culture (Fig. 7A, right) was observed after the 2-week culture under neutral conditions (Fig. 7B, right). These results indicate that LAM/LM acts directly to CD4 T cells to enhance the generation of IFN-γ-producing cells under T_h1 culture conditions and that LAM/LM acts indirectly via DCs

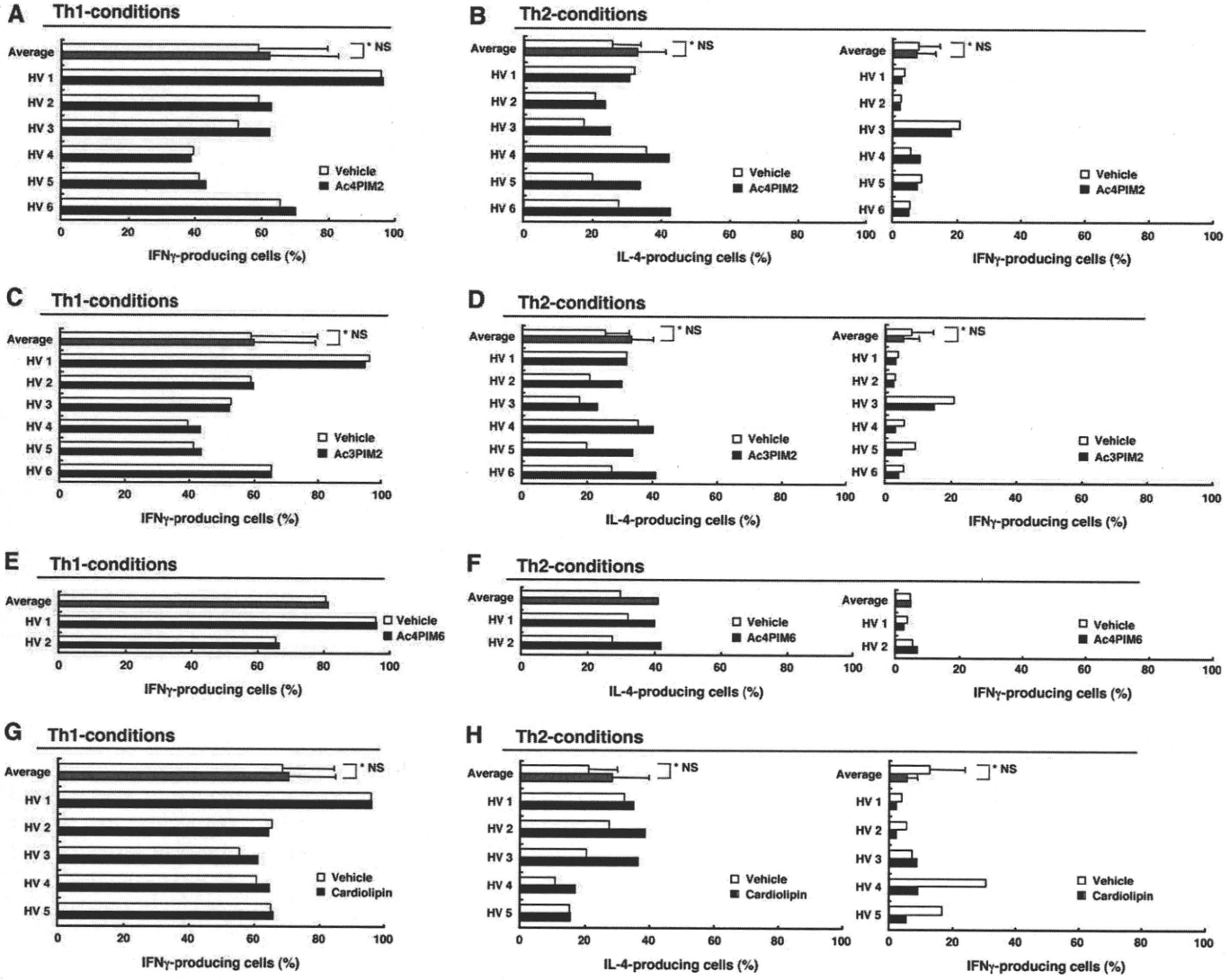

Fig. 5. Effect of Ac4PIM2, Ac3PIM2, Ac4PIM6 and cardiolipin on human T_h1/T_h2 differentiation. Effects of Ac4PIM2 under T_h1 (A) or T_h2 (B) conditions, Ac3PIM2 under T_h1 (C) or T_h2 (D) conditions, Ac4PIM6 under T_h1 (E) or T_h2 (F) conditions and cardiolipin under T_h1 (G) or T_h2 (H) conditions in T_h1/T_h2 differentiation are shown.

to CD4 T cells to enhance the generation of IFN-γ-producing cells and inhibit the generation of IL-4-producing cells under T_h2 culture conditions. IL-12 appears to play an important role in the indirect regulation by LAM/LM.

Effects of purified LAM and LM in human T_h1/T_h2 differentiation cultures

The balance of ManLAM/LM is considered to be important for the protection from mycobacterial infection (34). To further confirm the effects of LAM and LM on the T_h1/T_h2 differentiation, each component was purified from the mixture of LAM/LM and added into the T_h1/T_h2 cultures. Under T_h1 culture conditions, both LAM and LM enhanced the IFN-γ-producing T_h1 cells (58.8 versus 67.3 and 65.5%, respectively), although the levels were slightly lower than those of the cultures with LAM/LM mixture (83.0%; Fig. 8, upper panels). Under T_h2 culture conditions, LAM and LM also induced the generation of IFN-γ-producing T_h1 cells (18.1 versus 35.0 and 29.5%, respectively; Fig. 8, lower panels). No obvious inhibition of the generation of IL-4-producing cells was observed in the presence of LAM or LM. These results indicate that both LAM and LM components possess the ability to enhance T_h1 differentiation. In addition, the balance of LAM/LM may also contribute to the effect on T_h differentiation.

Discussion

The present study using an *in vitro* T_h1/T_h2 differentiation culture system with human peripheral blood naive CD4 T cells demonstrated that LAM/LM from *M. bovis* BCG enhanced T_h1 differentiation by two distinct pathways (Fig. 9). LAM/LM acts directly to naive CD4 T cells to enhance T_h1 cell differentiation under T_h1 culture conditions. LAM/LM also acts indirectly via DCs to induce polarization in T_h differentiation from T_h2 to T_h1 under T_h2 culture conditions.

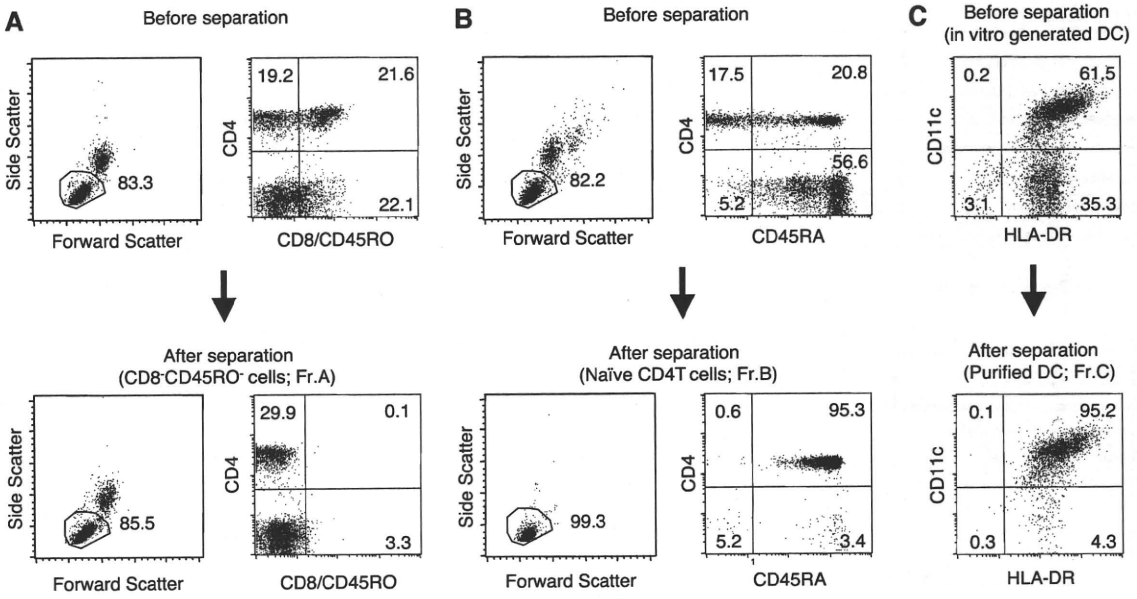

Fig. 6. Enrichment of human naive CD4 T cells and DCs. (A) Isolation of naive CD4 ($CD8^-CD45RO^-$) T cells (Fraction A). Human PBMCs were stained with FITC-conjugated anti-CD8 mAb, FITC-conjugated anti-CD45RO mAb and anti-FITC magnetic beads and then sorted the negative fraction using an AutoMACS® cell sorter. The percentages of cells in each gate are shown. (B) Isolation of purified CD4 T cells (Fr. B). Naive $CD4^+$ T cells were isolated from human PBMCs using human naive $CD4^+$ T cell isolation kit and AutoMACS® cell sorter. The purity of $CD4^+$ cells was 95.3%. (C) Purification of DCs from *in vitro*-generated DCs. *In vitro*-cultured DCs were stained with PE-conjugated anti-CD11c mAb, and the positive fraction of the anti-PE mAb-coupled magnetic beads were purified using an AutoMACS® cell sorter. The purity of the DCs was 95.2%.

It is reported in mouse system that TLRs recognize LMs, and TLR2 play important roles in the induction of type-I inflammatory responses (40–42). The signals via TLR2 induced the expression of CD1 and T cell activation (43). Gilleron *et al.* showed that PIM2 and PIM6, which are the anchor motif of LAM/LM, activate primary macrophages to secrete TNFα through TLR2, irrespective of their acylation pattern (44). These results suggest that PIM2 and PIM6 activate APC via TLR2. In the current study, however, PIM2 and PIM6 did not enhance T_h1 differentiation under T_h1 culture conditions, but enhanced T_h2 differentiation in some individuals under T_h2 culture conditions (Fig. 3C). These results suggest that PIM2 and PIM6 may negatively regulate T_h1 generation through the enhanced differentiation of T_h2 under T_h2 conditions. The discrepancies in the response of APC against PIM2 and PIM6 may be due to the difference in the physicochemical properties of micelle sizes or the solvent used between the PIM products of Gilleron *et al.* (44) and ours. The former PIMs are less polar than that of LAM/LM and produce larger micelle particles in the endocytotic process. In any event, it is likely that LAM/LM stimulates DCs via TLR2 and modifies the balance of T_h1/T_h2 differentiation.

To examine the cellular mechanisms underlying the effect of LAM/LM on the T_h1/T_h2 differentiation, the results with a crude naive CD4 T cell fraction and a highly purified naive CD4 T cell fraction after eliminating APCs were compared. Interestingly, the enhanced generation of T_h1 by LAM/LM under T_h1 culture conditions can be seen markedly in the absence of APCs, but the inhibition of T_h2 generation under T_h2 culture conditions is totally dependent on APCs (Fig. 7). Human CD4 T cells express various types of TLRs including TLR2, 5 and 7/8 (45). In another report, human naive CD4 T cells were found to express undetectable levels of TLR2 but the expression was significantly increased after anti-CD3 stimulation (46). The expression of TLRs was examined in our purified CD4 T cells and it was revealed that the purified CD4 T cells express substantial mRNA levels of TLR1, 2, 5, 7, 9 and 10 (Ito, T. and Nakayame, T., unpublished observation). Thus, it is likely that LAM/LM binds directly to one of these TLRs and induces polarization toward T_h1 differentiation. Recently, in a mouse system, stimulation through TLR2 on T_h1 cells was observed to induce IFN-γ production and proliferation, and this effect is augmented by IL-2 or IL-12 (47). Thus, it is likely that LAM/LM acts on early activated CD4 T cells and also on developing T_h1 in the culture and resulted in the polarized T_h1 differentiation.

In the cultures under neutral conditions, the cytokine autoregulatory loops may proceed, and the effects observed under neutral conditions may be more reflective of the *in vivo* effects of LAM/LM. Unfortunately, in human CD4 T cell cultures, the differentiation of naive T cells into T_h1/T_h2 cells was not efficiently observed under neutral conditions, and no obvious effect of LAM/LM was detected (Figs 3 and 7). However, we observed increases in the generation of IFN-γ-producing cells when we added DCs to the purified CD4 T cell cultures (Fig. 7). Based on these results, we concluded that even under neutral conditions, LAM/LM has an enhancing effect on the generation of IFN-γ-producing T_h1. We will investigate the effect of LAM/LM in the presence of various kinds of DCs under neutral conditions in the near future.

It is possible that NKT cells play a role in the observed LAM/LM-mediated induction of T_h1 differentiation (48, 49). However, during the process of the magnetic separation of $CD8^-CD45RO^-$ cells (naive CD4 T cells, Fr. A in Fig. 6A), all

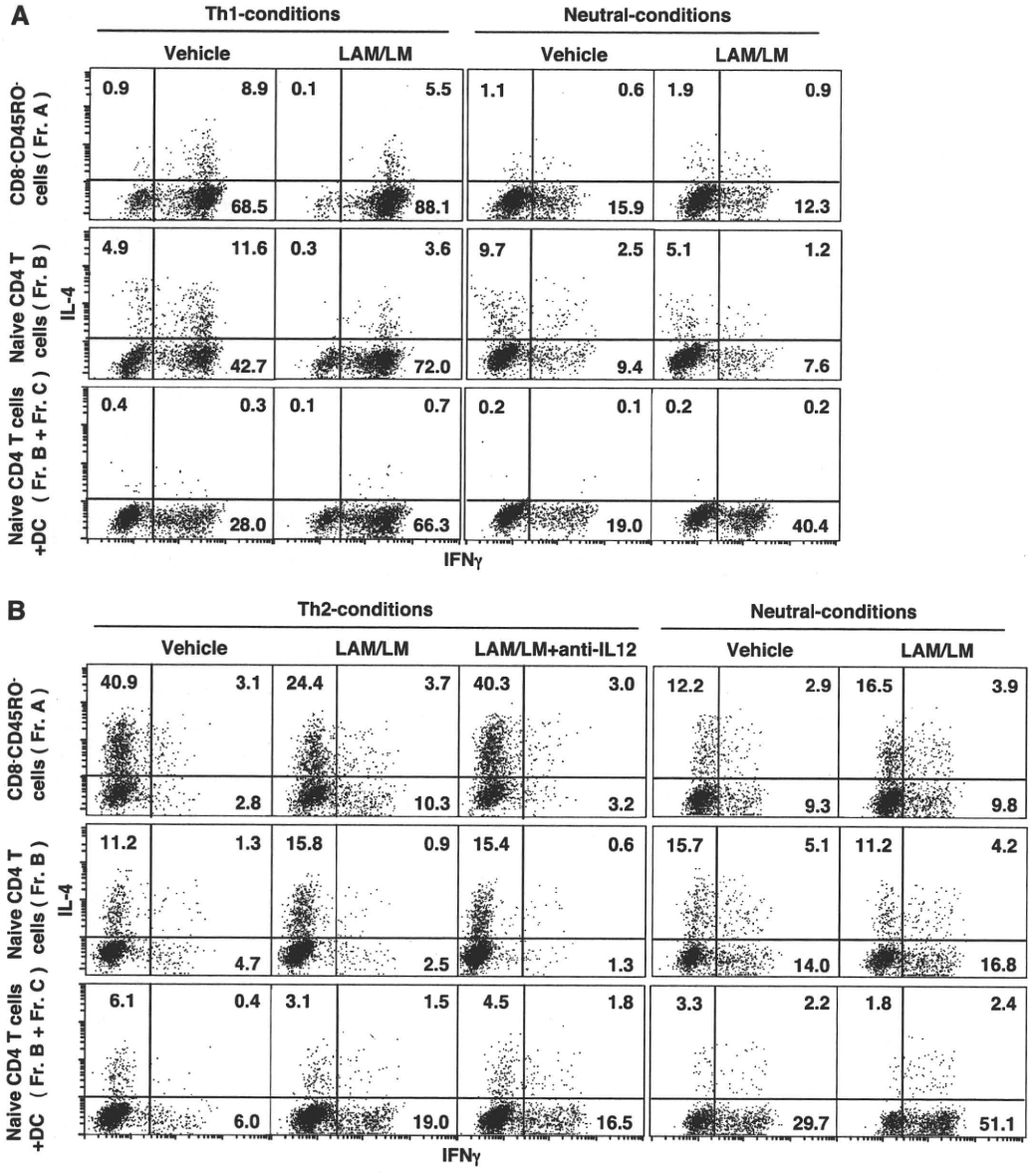

Fig. 7. Roles of DCs in the effect of LAM/LM on T_h1/T_h2 differentiation. Naive CD4 T cells ($CD8^-CD45RO^-$ cells) (Fr. A), purified CD4 T cells (Fr. B) and purified CD4 T cells (Fr. B) and DCs (Fr. C) were stimulated with anti-CD3 under T_h1 (panel A, cultured for a week), T_h2 (panel B, cultured for 2 weeks) or neutral culture conditions (panels A and B, cultured for 1 or 2 weeks, respectively). Anti-IL-12 mAb was added at the beginning of T_h2 cultures. Intracellular staining profiles of IFN-γ/IL-4 are shown with percentages of cells in each area. Three experiments were performed with similar results.

Vα24 NKT cells appeared to be eliminated and undetectable in our preparing naive CD4 T cells (Ito, T. and Nakayama, T., unpublished observation). Therefore, it is unlikely that Vα24 NKT cells are involved in the LAM/LM-mediated induction of T_h1 differentiation.

There are three types of capping motifs in LAM molecules. One is named ManLAM having a mannosyl cap, and this is isolated from *M. tuberculosis* and *M. bovis* including BCG subspecies and *Mycobacterium kansasii*. Another is PILAM, which has a phosphoinositol cap, and is isolated from *M. smegmatis*. The third one is AraLAM, which has no capping motif, and is isolated from *Mycobacterium chelonae* (44). It is reported that LAM and PILAM but not ManLAM or AraLAM activate macrophages and DCs to secrete IL-12 (26, 50, 51). On the other hand, LM but not PIM induces apoptosis or activates these cells to secrete IL-12 (25, 52). These results may indicate that ManLAM possesses the ability to inhibit LM-induced apoptosis and IL-12 secretion. In the present study, both LAM and LM components showed the enhancing activity of T_h1 differentiation (Fig. 8). However, we did not detect any inhibiting effects on the generation of IL-4-producing T_h2 (Fig. 8). We think that the inhibition of the generation of IL-4-secreting cells is a secondary effect by the enhancement of the generation of IFN-γ-producing cells because the inhibition was neutralized by the addition of anti-IL-12 mAb (Fig. 7). Since the effects of LAM and LM on the generation of IFN-γ-producing cells were milder than LAM/LM, we may not be able to detect the inhibition of the

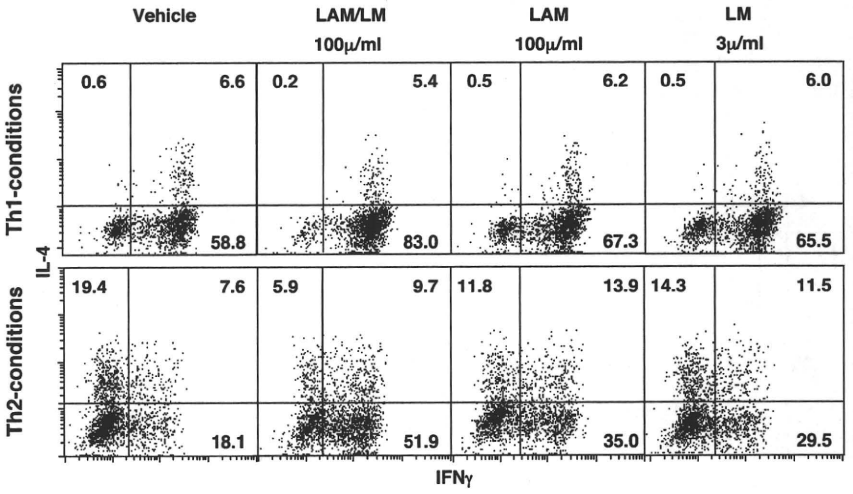

Fig. 8. Effects of purified LAM or LM components on human PBMC T_h1/T_h2 differentiation. Naive CD4 T cells from human PBMC were cultured with LAM/LM (100 μg ml^{-1}), LAM (30 and 100 μg ml^{-1}) or LM (3 and 30 μg ml^{-1}) under T_h1/T_h2 cultured conditions. The intracellular staining profiles of IFN-γ/IL-4 are shown with percentages of cells in each area. Three experiments were performed with similar results.

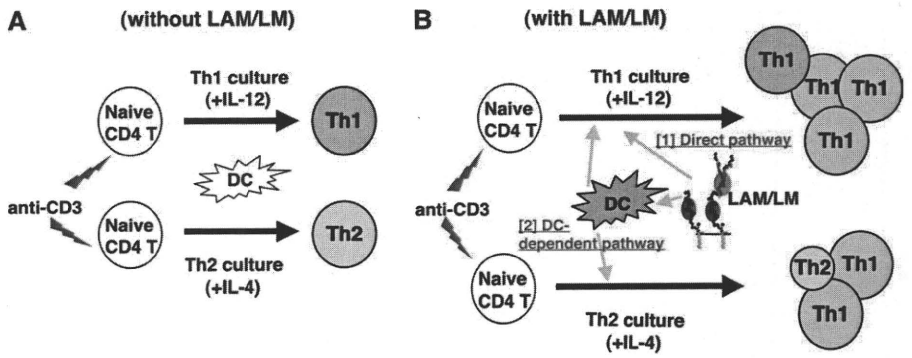

Fig. 9. Two distinct regulatory pathways for T_h1 generation induced by LAM/LM in human T_h1/T_h2 cultures. In the presence of LAM/LM, the generation of T_h1 cells was enhanced both under T_h1 culture conditions and T_h2 culture conditions (panel B). Under T_h1 conditions, LAM/LM directly act on CD4 T cells (direct pathway). LAM/LM act on DCs (DC-dependent pathway) and then induce the enhancement of T_h1 differentiation under both T_h1 and T_h2 conditions.

production of IL-4-secreting cells by LAM or LM (Fig. 8). LM appears to induce T_h1 differentiation more prominently in lower doses than LAM (Ito, T., and Nakayama, T., unpublished observation). In addition, high doses of LM did not show the enhancing effect in T_h1 differentiation (Ito, T., and Nakayama, T., unpublished observation). These results may suggest that the balance of LAM/LM is critically important for the induction of T_h1 responses. Further investigations on the effect of the balance of LAM/LM in the human immune system may contribute to the development of new immunotherapeutic approaches for allergic diseases, cancer and infections diseases.

Supplementary data

Supplementary Figure 1 available at *International Immunology* Online.

Funding

Ministry of Education, Culture, Sports, Science and Technology (Japan) [Grants-in-Aid: for Scientific Research on Priority Areas #17016010; Scientific Research (B) #17390139, Scientific Research (C) #18590466, #19590491 and #19591609, Exploratory Research #19659121 and Young Scientists (Start-up) #18890046; Special Coordination Funds for Promoting Science and Technology and Cancer Translational Research Project]; Ministry of Health, Labor and Welfare (Japan); The Japan Health Science Foundation; Kanae Foundation; Uehara Memorial Foundation; Mochida Foundation; Yasuda Medical Foundation; Astellas Foundation; Sagawa Foundation.

Acknowledgements

We thank Kaoru Sugaya, Hikari Asou and Satoko Norikane for their excellent technical assistance.

Abbreviations

APC	antigen presenting cell
BCG	Bacille Calmett–Guerin
CW	cell wall
DC	dendritic cell
LAM	lipoarabinomannan

LM	lipomannan
ManLAM	LAM with mannose caps
PI	phosphatidylinositol
PIM	phosphatidylinositol mannosides
PIM2	phosphatidylinositol dimannoside
PIM6	phosphatidylinositol hexamannoside
TLR2	Toll-like receptor 2
TNFα	tumor necrosis factor α

References

1 Besra, G. S., Morehouse, C. B., Rittner, C. M., Waechter, C. J. and Brennan, P. J. 1997. Biosynthesis of mycobacterial lipoarabinomannan. *J. Biol. Chem.* 272:18460.

2 Nigou, J., Gilleron, M. and Puzo, G. 1999. Lipoarabinomannans: characterization of the multiacylated forms of the phosphatidyl-*myo*-inositol anchor by NMR spectroscopy. *Biochem. J.* 337:453.

3 Sibley, L. D., Hunter, S. W., Brennan, P. J. and Krahenbuhl, J. L. 1988. Mycobacterial lipoarabinomannan inhibits gamma interferon-mediated activation of macrophages. *Infect. Immun.* 56:1232.

4 Sibley, L. D., Adams, L. B. and Krahenbuhl, J. L. 1990. Inhibition of interferon-gamma-mediated activation in mouse macrophages treated with lipoarabinomannan. *Clin. Exp. Immunol.* 80:141.

5 Moreno, C., Mehlert, A. and Lamb, J. 1988. The inhibitory effects of mycobacterial lipoarabinomannan and polysaccharides upon polyclonal and monoclonal human T cell proliferation. *Clin. Exp. Immunol.* 74:206.

6 Chan, J., Fan, X. D., Hunter, S. W., Brennan, P. J. and Bloom, B. R. 1991. Lipoarabinomannan, a possible virulence factor involved in persistence of *Mycobacterium tuberculosis* within macrophages. *Infect. Immun.* 59:1755.

7 Schlesinger, L. S., Hull, S. R. and Kaufman, T. M. 1994. Binding of the terminal mannosyl units of lipoarabinomannan from a virulent strain of *Mycobacterium tuberculosis* to human macrophages. *J. Immunol.* 152:4070.

8 Apostolou, I., Takahama, Y., Belmant, C. *et al.* 1999. Murine natural killer T(NKT) cells [correction of natural killer cells] contribute to the granulomatous reaction caused by mycobacterial cell walls. *Proc. Natl Acad. Sci. USA* 96:5141.

9 Gilleron, M., Ronet, C., Mempel, M., Monsarrat, B., Gachelin, G. and Puzo, G. 2001. Acylation state of the phosphatidylinositol mannosides from *Mycobacterium bovis* bacillus Calmette Guerin and ability to induce granuloma and recruit natural killer T cells. *J. Biol. Chem.* 276:34896.

10 Khoo, K. H., Dell, A., Morris, H. R., Brennan, P. J. and Chatterjee, D. 1995. Structural definition of acylated phosphatidylinositol mannosides from *Mycobacterium tuberculosis*: definition of a common anchor for lipomannan and lipoarabinomannan. *Glycobiology.* 5:117.

11 Schaeffer, M. L., Khoo, K. H., Besra, G. S. *et al.* 1999. The *pimB* gene of *Mycobacterium tuberculosis* encodes a mannosyltransferase involved in lipoarabinomannan biosynthesis. *J. Biol. Chem.* 274:31625.

12 Kremer, L., Gurcha, S. S., Bifani, P. *et al.* 2002. Characterization of a putative α-mannosyltransferase involved in phosphatidylinositol trimannoside biosynthesis in *Mycobacterium tuberculosis*. *Biochem. J.* 363:437.

13 Hunter, S. W. and Brennan, P. J. 1990. Evidence for the presence of a phosphatidylinositol anchor on the lipoarabinomannan and lipomannan of *Mycobacterium tuberculosis*. *J. Biol. Chem.* 265:9272.

14 Banchereau, J. and Steinman, R. M. 1998. Dendritic cells and the control of immunity. *Nature* 392:245.

15 Cella, M., Sallusto, F. and Lanzavecchia, A. 1997. Origin, maturation and antigen presenting function of dendritic cells. *Curr. Opin. Immunol.* 9:10.

16 Reis e Sousa, C., Sher, A. and Kaye, P. 1999. The role of dendritic cells in the induction and regulation of immunity to microbial infection. *Curr. Opin. Immunol.* 11:392.

17 Demangel, C., Bean, A. G., Martin, E., Feng, C. G., Kamath, A. T. and Britton, W. J. 1999. Protection against aerosol *Mycobacterium tuberculosis* infection using *Mycobacterium bovis* Bacillus Calmette Guerin-infected dendritic cells. *Eur. J. Immunol.* 29:1972.

18 Thurnher, M., Ramoner, R., Gastl, G. *et al.* 1997. Bacillus Calmette-Guerin mycobacteria stimulate human blood dendritic cells. *Int. J. Cancer.* 70:128.

19 Tascon, R. E., Soares, C. S., Ragno, S., Stavropoulos, E., Hirst, E. M. and Colston, M. J. 2000. *Mycobacterium tuberculosis*-activated dendritic cells induce protective immunity in mice. *Immunology.* 99:473.

20 Cooper, A. M., Dalton, D. K., Stewart, T. A., Griffin, J. P., Russell, D. G. and Orme, I. M. 1993. Disseminated tuberculosis in interferon γ gene-disrupted mice. *J. Exp. Med.* 178:2243.

21 Flynn, J. L., Chan, J., Triebold, K. J., Dalton, D. K., Stewart, T. A. and Bloom, B. R. 1993. An essential role for interferon γ in resistance to *Mycobacterium tuberculosis* infection. *J. Exp. Med.* 178:2249.

22 Dalton, D. K., Haynes, L., Chu, C. Q., Swain, S. L. and Wittmer, S. 2000. Interferon γ eliminates responding CD4 T cells during mycobacterial infection by inducing apoptosis of activated CD4 T cells. *J. Exp. Med.* 192:117.

23 Li, X., McKinstry, K. K., Swain, S. L. and Dalton, D. K. 2007. IFN-γ acts directly on activated $CD4^+$ T cells during mycobacterial infection to promote apoptosis by inducing components of the intracellular apoptosis machinery and by inducing extracellular proapoptotic signals. *J. Immunol.* 179:939.

24 Ottenhoff, T. H., Kumararatne, D. and Casanova, J. L. 1998. Novel human immunodeficiencies reveal the essential role of type-I cytokines in immunity to intracellular bacteria. *Immunol. Today.* 19:491.

25 Nigou, J., Zelle-Rieser, C., Gilleron, M., Thurnher, M. and Puzo, G. 2001. Mannosylated lipoarabinomannans inhibit IL-12 production by human dendritic cells: evidence for a negative signal delivered through the mannose receptor. *J. Immunol.* 166:7477.

26 Geijtenbeek, T. B., Van Vliet, S. J., Koppel, E. A. *et al.* 2003. Mycobacteria target DC-SIGN to suppress dendritic cell function. *J. Exp. Med.* 197:7.

27 Tailleux, L., Maeda, N., Nigou, J., Gicquel, B. and Neyrolles, O. 2003. How is the phagocyte lectin keyboard played? Master class lesson by *Mycobacterium tuberculosis*. *Trends Microbiol.* 11:259.

28 Gilleron, M., Himoudi, N., Adam, O. *et al.* 1997. *Mycobacterium smegmatis* phosphoinositols-glyceroarabinomannans. Structure and localization of alkali-labile and alkali-stable phosphoinositides. *J. Biol. Chem.* 272:117.

29 Adams, L. B., Fukutomi, Y. and Krahenbuhl, J. L. 1993. Regulation of murine macrophage effector functions by lipoarabinomannan from mycobacterial strains with different degrees of virulence. *Infect. Immun.* 61:4173.

30 Means, T. K., Lien, E., Yoshimura, A., Wang, S., Golenbock, D. T. and Fenton, M. J. 1999. The CD14 ligands lipoarabinomannan and lipopolysaccharide differ in their requirement for Toll-like receptors. *J. Immunol.* 163:6748.

31 Vignal, C., Guerardel, Y., Kremer, L. *et al.* 2003. Lipomannans, but not lipoarabinomannans, purified from *Mycobacterium chelonae* and *Mycobacterium kansasii* induce TNF-α and IL-8 secretion by a CD14-toll-like receptor 2-dependent mechanism. *J. Immunol.* 171:2014.

32 Quesniaux, V. J., Nicolle, D. M., Torres, D. *et al.* 2004. Toll-like receptor 2 (TLR2)-dependent-positive and TLR2-independent-negative regulation of proinflammatory cytokines by mycobacterial lipomannans. *J. Immunol.* 172:4425.

33 Dao, D. N., Kremer, L., Guerardel, Y. *et al.* 2004. *Mycobacterium tuberculosis* lipomannan induces apoptosis and interleukin-12 production in macrophages. *Infect. Immun.* 72:2067.

34 Briken, V., Porcelli, S. A., Besra, G. S. and Kremer, L. 2004. Mycobacterial lipoarabinomannan and related lipoglycans: from biogenesis to modulation of the immune response. *Mol. Microbiol.* 53:391.

35 Fujita, Y., Doi, T., Sato, K. and Yano, I. 2005. Diverse humoral immune responses and changes in IgG antibody levels against mycobacterial lipid antigens in active tuberculosis. *Microbiology.* 151:2065.

36 Nigou, J., Gilleron, M., Cahuzac, B. *et al.* 1997. The phosphatidyl-*myo*-inositol anchor of the lipoarabinomannans from *Mycobacterium*

bovis bacillus Calmette Guerin. Heterogeneity, structure, and role in the regulation of cytokine secretion. *J. Biol. Chem.* 272:23094.
37 Motohashi, S., Kobayashi, S., Ito, T. *et al.* 2002. Preserved IFN-α production of circulating Vα24 NKT cells in primary lung cancer patients. *Int. J. Cancer.* 102:159.
38 Ishikawa, E., Motohashi, S., Ishikawa, A. *et al.* 2005. Dendritic cell maturation by CD11c− T cells and $V\alpha24^+$ natural killer T-cell activation by α-galactosylceramide. *Int. J. Cancer.* 117:265.
39 Kaneko, T., Hosokawa, H., Yamashita, M. *et al.* 2007. Chromatin remodeling at the Th2 cytokine gene loci in human type 2 helper T cells. *Mol. Immunol.* 44:2249.
40 Fricke, I., Mitchell, D., Mittelstadt, J. *et al.* 2006. Mycobacteria induce IFN-γ production in human dendritic cells via triggering of TLR2. *J. Immunol.* 176:5173.
41 Gilleron, M., Nigou, J., Nicolle, D., Quesniaux, V. and Puzo, G. 2006. The acylation state of mycobacterial lipomannans modulates innate immunity response through toll-like receptor 2. *Chem. Biol.* 13:39.
42 Dabbagh, K. and Lewis, D. B. 2003. Toll-like receptors and T-helper-1/T-helper-2 responses. *Curr. Opin. Infect. Dis.* 16:199.
43 Roura-Mir, C., Wang, L., Cheng, T. Y. *et al.* 2005. *Mycobacterium tuberculosis* regulates CD1 antigen presentation pathways through TLR-2. *J. Immunol.* 175:1758.
44 Nigou, J., Gilleron, M. and Puzo, G. 2003. Lipoarabinomannans: from structure to biosynthesis. *Biochimie.* 85:153.
45 Kabelitz, D. 2007. Expression and function of Toll-like receptors in T lymphocytes. *Curr. Opin. Immunol.* 19:39.
46 Xu, D., Komai-Koma, M. and Liew, F. Y. 2005. Expression and function of Toll-like receptor on T cells. *Cell. Immunol.* 233:85.
47 Imanishi, T., Hara, H., Suzuki, S., Suzuki, N., Akira, S. and Saito, T. 2007. Cutting edge: tLR2 directly triggers Th1 effector functions. *J. Immunol.* 178:6715.
48 Emoto, M., Emoto, Y., Buchwalow, I. B. and Kaufmann, S. H. 1999. Induction of IFN-γ-producing $CD4^+$ natural killer T cells by *Mycobacterium bovis* bacillus Calmette Guerin. *Eur. J. Immunol.* 29:650.
49 Dieli, F., Taniguchi, M., Kronenberg, M. *et al.* 2003. An anti-inflammatory role for Vα14 NK T cells in *Mycobacterium bovis* bacillus Calmette-Guerin-infected mice. *J. Immunol.* 171:1961.
50 Rojas, M., Garcia, L. F., Nigou, J., Puzo, G. and Olivier, M. 2000. Mannosylated lipoarabinomannan antagonizes *Mycobacterium tuberculosis*-induced macrophage apoptosis by altering Ca^{+2}-dependent cell signaling. *J. Infect. Dis.* 182:240.
51 Yoshida, A. and Koide, Y. 1997. Arabinofuranosyl-terminated and mannosylated lipoarabinomannans from *Mycobacterium tuberculosis* induce different levels of interleukin-12 expression in murine macrophages. *Infect. Immun.* 65:1953.
52 Nigou, J., Gilleron, M., Rojas, M., Garcia, L. F., Thurnher, M. and Puzo, G. 2002. Mycobacterial lipoarabinomannans: modulators of dendritic cell function and the apoptotic response. *Microbes Infect.* 4:945.

THE JOURNAL OF BIOLOGICAL CHEMISTRY VOL. 283, NO. 43, pp. 28835–28841, October 24, 2008

Mycolyltransferase-mediated Glycolipid Exchange in Mycobacteria*

Received for publication, July 28, 2008, and in revised form, August 14, 2008 Published, JBC Papers in Press, August 14, 2008, DOI 10.1074/jbc.M805776200

Isamu Matsunaga[‡§], Takashi Naka[¶], Rahul S. Talekar[‖], Matthew J. McConnell[‖], Kumiko Katoh[‡§], Hitomi Nakao[‡§], Atsushi Otsuka[‡], Samuel M. Behar[‖], Ikuya Yano[¶], D. Branch Moody[‖], and Masahiko Sugita[‡§1]

From the [‡]Laboratory of Cell Regulation, Institute for Virus Research and [§]Laboratory of Cell Regulation and Molecular Network, Graduate School of Biostudies, Kyoto University, Kyoto 606-8507, Japan, [¶]Japan BCG Laboratory, Tokyo 204-0022, Japan, and [‖]Division of Rheumatology, Immunology, and Allergy, Brigham and Women's Hospital, Harvard Medical School, Boston, Massachusetts 02115

Trehalose dimycolate (TDM), also known as cord factor, is a major surface glycolipid of the cell wall of mycobacteria. Because of its potent biological functions in models of infection, adjuvancy, and immunotherapy, it is important to determine how its biosynthesis is regulated. Here we show that glucose, a host-derived product that is not readily available in the environment, causes *Mycobacterium avium* to down-regulate TDM expression while up-regulating production of another major glycolipid with immunological roles in T cell activation, glucose monomycolate (GMM). *In vitro*, the mechanism of reciprocal regulation of TDM and GMM involves competitive substrate selection by antigen 85A. The switch from TDM to GMM biosynthesis occurs near the physiological concentration of glucose present in mammalian hosts. We further demonstrate that GMM is produced *in vivo* by mycobacteria growing in mouse lung. These results establish an enzymatic pathway for GMM production. More generally, these observations provide a specific enzymatic mechanism for dynamic alterations of cell wall glycolipid remodeling in response to the transition from noncellular to cellular growth environments, including factors that are monitored by the host immune system.

Mycobacterium avium complex (MAC)[2] includes a group of acid-fast bacteria that distribute widely in natural environments, including soil, water, aerosols, and dust (1). Although less virulent than *Mycobacterium tuberculosis*, these environmental mycobacteria occasionally infect humans, especially patients infected with human immunodeficiency virus type 1, where they represent a major cause of morbidity. The incidence of clinically overt MAC infection has increased significantly in recent years, and because of the multidrug resistance evolved by the microbes, MAC infection is difficult to clear with chemotherapeutic agents. Thus, *M. tuberculosis* and MAC are now the two major groups of mycobacteria species that require further efforts for prevention and treatment. Unlike *M. tuberculosis*, which transmits primarily from individuals with active disease, epidemiologic evidence suggests that such transmission pathways are unlikely for MAC. Rather, MAC infection appears to occur when susceptible individuals are exposed to environmental MAC. These observations predict that, upon infection, environmental MAC should undergo significant adaptive changes to allow its survival and replication within the host.

Mycobacteria possess highly lipid-rich cell walls that are critical not simply for their acid-fast properties but also for their survival and replication. The cell wall contains mycolic acids, an α-alkyl-β-hydroxy fatty acid with extremely long carbon chains ($\sim C_{80}$), which are densely aligned in covalent association with the 6-position of arabinose termini of the underlying arabinogalactan sugar layer or exist as free molecules complexed to sugars, either glucose or trehalose. Arabinogalactan-linked mycolates are proposed to extend outward and interact noncovalently with carbon chains of the so-called surface-exposed glycolipids, including trehalose 6-monomycolate (TMM), trehalose 6,6′-dimycolate (TDM), and glucose 6-monomycolate (GMM), thereby forming the hydrophobic cell wall architecture that is essential for protection against chemical attack, such as reactive oxygen intermediates and hydrolytic enzymes derived from the host cells. Among the most abundant surface-exposed glycolipids is TDM that is biosynthesized from its precursor, TMM, by the mycolyltransferase activity of antigen 85 (Ag85) (2). Many biological functions have been assigned to TDM (3) that may impact on survival of mycobacteria within the host and possibly their virulence. Therefore, it is important to determine how biosynthesis of TDM and other mycolic acid-containing glycolipids is regulated by external factors. GMM exists at varied levels in the mycobacterial cell wall (4, 5). In addition to its role in cell wall barrier functions, GMM is a granuloma-forming agent in mice (6) as well as a CD1b presented antigen in humans (7).

* This work was supported, in whole or in part, by National Institutes of Health Grant R01 07155 (NIAID) (to D. B. M.). This work was also supported by grants-in-aid from scientific research on priority areas from the Ministry of Education, Culture, Sports, Science and Technology (to M. S.), grants-in-aid for scientific research B (to M. S.) and C (to I. M.) from the Japan Society for the Promotion of Science, grants from the Ministry of Health, Labour, and Welfare Research on Emerging and Re-emerging Infectious Diseases (to M. S.), and by the Burroughs Wellcome Fund (to D. B. M.). The costs of publication of this article were defrayed in part by the payment of page charges. This article must therefore be hereby marked "*advertisement*" in accordance with 18 U.S.C. Section 1734 solely to indicate this fact.

The nucleotide sequence(s) reported in this paper has been submitted to the DDBJ/GenBank™/EBI Data Bank with accession number(s) AB325677.

[1] To whom correspondence should be addressed: 53 Kawahara-cho, Shogoin, Sakyo-ku, Kyoto 606-8507, Japan. Fax: 81-75-752-3232; E-mail: msugita@virus.kyoto-u.ac.jp.

[2] The abbreviations used are: MAC, *Mycobacterium avium* complex; Ag85, antigen 85; GC-MS, gas chromatography-mass spectrometry; GMM, glucose 6-monomycolate; IL-2, interleukin-2; MALDI-TOF MS, matrix-assisted laser desorption ionization-time of flight mass spectrometry; TCR, T cell receptor; TDM, trehalose 6,6′-dimycolate; TMM, trehalose 6-monomycolate; LC-MS, liquid chromatography-mass spectrometry.

Here we identify Ag85A as an enzyme that produces GMM by transfer of mycolate to glucose. Furthermore, mechanistic studies show that glucose present in its growth environment regulates the spectrum of mycolylglycolipids made by MAC, and glucose from the host influences GMM production *in vivo* during infection of mice. Mechanistic studies showed that glucose and trehalose compete as substrates for Ag85A, linking the biosynthesis pathways of GMM and TDM.

EXPERIMENTAL PROCEDURES

Reagents and Bacteria—Chemical reagents were purchased from Nacalai Tesque (Kyoto, Japan) unless otherwise indicated. *M. avium* ATCC 35767 (serovar 4) was obtained from American Type Culture Collection (Manassas, VA). The bacteria were maintained on a plate of Middlebrook 7H10 media supplemented with 10% oleic acid/albumin/dextrose/catalase (BD Biosciences). For extraction of the total lipid fraction, the bacteria were cultured in Middlebrook 7H9 broth media (containing 0.05% Tween 80 but not glycerol) supplemented with 10% albumin/dextrose/catalase (BD Biosciences). The log phase culture was diluted with 20 volumes of 7H9 media containing various concentrations of glucose, and the culture was continued for another 5–7 days until the absorbance at 600 nm reached ~1. In some experiments, bacteria were grown in media containing either 0.01 or 0.1% glucose, and the media were replaced every day with fresh media containing the same concentrations of glucose. After 5 days, the bacteria were harvested for lipid extraction. To monitor early GMM production, bacteria were grown either in 7H9 media containing 0.01 or 0.1% glucose or in human serum and were harvested after 2, 4, 8, 18, and 24 h of culture.

Preparation of Mycolylglycolipids from MAC—Total lipids from mycobacteria were prepared as described previously (8). The total lipids were then dissolved in chloroform/methanol (C/M, 2:1, v/v), and 20 volumes of ice-cold acetone were added. After 30 min of incubation on ice, the suspension was subjected to centrifugation at 1,500 × *g* for 15 min at 1 °C, and the supernatant was carefully removed. The pellet was then washed with ice-cold acetone, and the residue was dissolved in C/M (2:1) and fractionated by TLC using an Analtech TLC plate (Newark, DE) with a solvent system of chloroform/methanol/acetone/acetic acid (90:10:10:1, v/v). GMM, TDM and TMM fractions were extracted with C/M (2:1) from the silica gels. For GMM and TDM purification, the fractions were further fractionated by TLC with a solvent system of chloroform/acetone/methanol/water (50:60:2.5:0.6, v/v). Finally, the GMM, TDM and TMM fractions were extracted with C/M (2:1), dried, and rinsed several times with methanol at room temperature to remove any residual contamination of glycopeptidolipids and phospholipids.

Matrix-assisted Laser Desorption Ionization-Time of Flight Mass Spectrometry (MALDI-TOF MS)—MALDI-TOF MS analyses of glycolipids were carried out according to the method described previously (9). Briefly, MALDI-TOF MS spectra were acquired on a Voyager DE-STR MALDI-TOF mass spectrometer (Applied Biosystems) with a pulse laser emitting at 337 nm. Samples were analyzed in the reflectron mode with an accelerating voltage operating in positive ion mode of 20 kV. As the matrix, 2,5-dihydroxybenzoic acid was used.

Gas Chromatography-Mass Spectrometry (GC-MS)—GC-MS analysis of the sugar moiety of GMM was carried out according to the method described previously (9). Briefly, GMM was hydrolyzed with 2 M trifluoroacetic acid at 120 °C for 2 h. The aqueous phase was dried, reduced with 10 mg/ml solution of $NaBD_4$ (1 M NH_4OH/C_2H_5OH, 1:1, v/v) at room temperature for 2 h, and then acetylated with acetic anhydride/pyridine (1:1, v/v) at 100 °C for 1 h. The resulting alditol acetate derivatives were analyzed by GC-MS with GCMS-QP2010 plus (Shimazu Co., Ltd., Kyoto, Japan), using a fused silica capillary column (SP-2380, 30 m × 0.25 mm inner diameter; Supelco Inc.). GC oven was operated at 50 °C for 0.5 min, and then the temperature was increased to 235 °C at a rate of 65 °C/s. The temperature was then kept at 235 °C for 12 min. Flow rate of helium gas was 44.4 cm/min.

Isolation of the Antigen 85A Gene from MAC, Preparation of the Recombinant Enzyme and Its Enzymatic Assay—The genomic DNA was isolated from the MAC strain using the Isoplant kit according to the manufacturer's instruction (Wako Pure Chemical Co. Ltd., Osaka, Japan). The gene that encoded the mature Ag85A lacking the signal sequence was amplified by PCR, using a specific primer set as follows: 5′-gga att cca tat gtt ctc gcg ccc cgg tct gcc-3′ (a sense primer, in which the NdeI restriction site is underlined) and 5′-ccg ctc gag ggt gcc ctgg ccg ttc ccg g-3′ (an antisense primer, in which the XhoI restriction site is underlined). PCR was carried out using a Takara LA-*Taq*DNA polymerase (Takara Co. Ltd., Tokyo, Japan), and the cycling conditions for PCR amplification were as follows: 94 °C, 2 min, followed by 30 cycles of 98 °C, 20 s and 72 °C, 1.5 min, and a final extension step of 72 °C, 3 min. The amplified PCR products were digested with NdeI and XhoI and ligated to a NdeI-XhoI-digested pET-21c plasmid vector (Merck). The nucleotide sequences of the Ag85A gene were determined for four isolated clones. *Escherichia coli* BL21 (DE3) was transformed with the Ag85A gene in pET-21c, and induction of protein expression was performed according to a method of Kremer *et al.* (10).

The bacteria expressing the His-tagged mature Ag85A were harvested and disrupted by sonication in ice-cold 20 mM Tris-HCl buffer (pH 7.9) containing 0.5 M NaCl and 60 mM imidazole (sonication buffer). The sonicate was centrifuged at 10,000 × *g* for 30 min at 4 °C to remove insoluble materials, and then the supernatant was applied onto a Ni^{2+}-resin column equilibrated with the sonication buffer at 4 °C. After washing the column with the sonication buffer, the recombinant Ag85A was eluted with 20 mM Tris-HCl buffer (pH 7.9) containing 0.5 M NaCl and 0.5 M imidazole. The eluate was concentrated and dialyzed against 50 mM Tris-HCl buffer (pH 7.4) containing 10% glycerol overnight at 4 °C. Protein concentration of the recombinant Ag85A preparation was determined by the Quick Start Bradford protein assay kit (Bio-Rad). Purity of the preparation was determined by SDS-PAGE and Coomassie staining.

Mycolyltransferase assays were carried out by modification of a method of Kremer *et al.* (10). Twenty μg of purified TMM was dispersed by sonication in 150 μl of 50 mM sodium phosphate buffer (pH 7.4) in the presence or absence of indicated

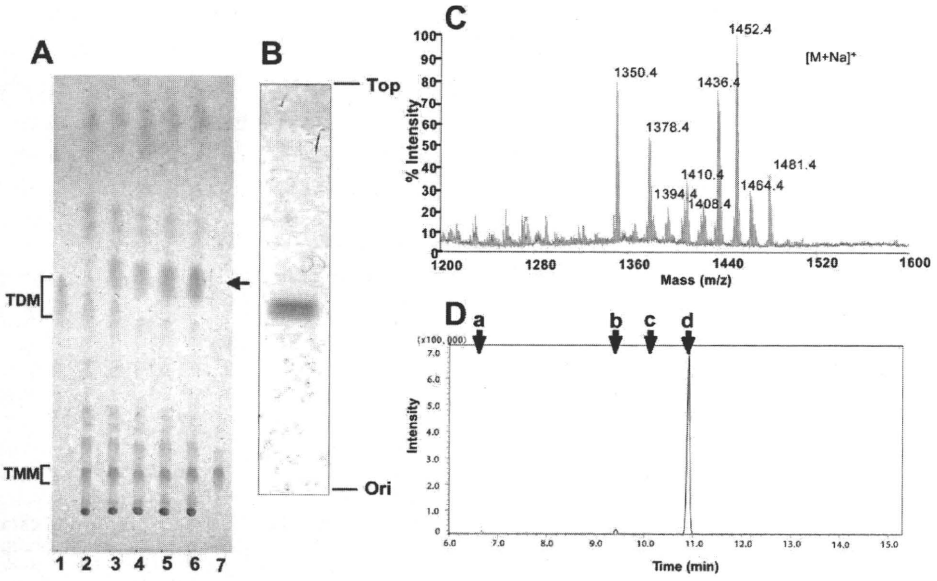

FIGURE 1. **A reciprocal production of TDM and GMM in MAC in response to glucose.** *A*, MAC was cultured in media containing 0.01% (w/v, *lane 2*), 1% (w/v, *lane 3*), 2% (w/v, *lane 4*), 5% (w/v, *lane 5*), and 10% glucose (w/v, *lane 6*), and the total lipid fractions (50 μg each) were analyzed on a TLC plate that was developed with chloroform/methanol/acetone/acetic acid (90:10:10:1, v/v). Purified TDM (*lane 1*) and TMM (*lane 7*) were used as references. Glucose dose-dependent production of a lipid species (indicated with an *arrow*) was detected. *B*, lipid species was purified and analyzed on a silica gel TLC plate that was developed with chloroform/methanol (9:1, v/v). *C*, MALDI-TOF MS profiles of the purified lipid species. *D*, GC-MS analysis of the sugar moiety of the purified lipid species. *Arrows* indicate retention times for the alditol acetate derivatives of arabinose (*a*), mannose (*b*), galactose (*c*)/ and glucose (*d*). Ion chromatogram of *m/z* 290 is shown. The retention time of the major ion corresponded with that of a glucose alditol acetate derivative.

concentration of D-glucose. The reaction was started by the addition of 50 μl of the enzyme preparation containing 50 μg of protein. After 1 h of incubation at 37 °C, the reaction was stopped by the addition of 2 ml of C/M (2:1) and 0.3 ml of distilled water. The lipids were extracted by the method of Kremer *et al.* (10) and analyzed by silica gel TLC. The lipids on the TLC plate were visualized by spraying 50% sulfuric acid and baking.

GMM Detection in Vivo—Mouse infections were carried out via the aerosol route with 10^2 *M. tuberculosis* Erdman strain with mice sacrificed after ~21 days of infection. Lungs were homogenized with beads and centrifuged at 2000 × *g* for 30 min at room temperature. The bacterial pellet was treated with 2% NaOH to disperse phospholipid bilayers, neutralized with 0.27 M phosphoric acid in phosphate buffered saline, and centrifuged at 2000 × *g* for 30 min to recover bacteria. Lipids were extracted from this mixture with three serial extractions in C/M (2:1, 1:1, and 1:2), evaporated to dryness under nitrogen, and resuspended in 1:1 C/M. These lipids were further fractionated by cold acetone precipitation to enrich for lipids that were analyzed by normal phase chromatography on a diol column. Solvent A was methanol, and solvent B was 60:40 (v/v) hexane/2-propanol. Both solvents contained 0.1% (v/v) formic acid and 0.05% (v/v) ammonium hydroxide. A binary gradient was used beginning at 5% solvent A for 3 min, linearly increasing to 40% solvent A over 5 min, holding at 40% solvent A for 6 min, linearly increasing to 100% solvent A over 2.2 min, holding at 100% solvent A for 3 min, linearly decreasing to 5% solvent A over 3.6 min, and finally holding at 5% solvent A for 3.2 min. Compounds matching the expected mass for GMM were detected at after 3.6–3.9 min of elution under these conditions. The accurate mass experiment was carried out with an Agilent 6520 Accurate Mass QTOF-LC-MS operated in the positive mode with an Agilent Technologies 1200 Series high pressure liquid chromatography system. CID-MS was carried out with a ThermoLCQ Advantage Ion Trap mass spectrometer with nano-electrospray ionization in comparison with GMM derived from *Mycobacterium fallax* (11).

GMM-specific T Cell Assays—The T cell receptor (TCR)-deficient Jurkat cells (J.RT3) reconstituted by transfection with GMM-specific, CD1b-restricted TCRs have been described previously (12). The T cells (5×10^4/well) were cocultured in 96-well microtiter plates with the C1R human B-lymphoblastoid cells (1×10^5/well) stably transfected either with CD1b (C1R/CD1b) or with empty vector alone (C1R/mock) (13) in the presence of phorbol 12-myristate 13-acetate (10 ng/ml) and indicated concentrations of lipid preparations. In some experiments, monocyte-derived dendritic cells were used as antigen-presenting cells. After 20 h, aliquots of the culture supernatants were collected, and the amount of interleukin-2 (IL-2) released into the supernatants was measured by the IL-2 ELISA kit (BD Biosciences).

RESULTS

Reciprocal Production of TDM and GMM by MAC in Response to Glucose—Glucose is an essential nutrient to living organisms, which is utilized as a source not only for energy production but also for biosynthesis of glycosylated constituents of cellular architecture. Unlike other hexose sugars, glucose is maintained at high levels in the blood and tissues of mammalian hosts. Therefore, we predicted that, upon infection into the host, MAC grown in glucose-limited environments might undergo significant alterations in glycolipid biosynthesis by exposure to host-derived glucose. To gain insights into the impact of exogenous glucose on glycolipid composition in mycobacteria, we first monitored glycolipid production by *M. avium* strain (serovar 4) that was harvested after cultivation in liquid media supplemented with different concentrations of glucose. The total lipid fraction was obtained by extracting each bacterial preparation with chloroform and methanol. The lipids were then analyzed on a TLC plate developed with a solvent system suitable for separation of chemically diverse glycolipid species (Fig. 1*A*). When grown in the presence of a trace amount of glucose (0.01%, w/v), mycobacteria produced high levels of TDM and TMM (Fig. 1*A*, *lane 2*, shown with *brackets*). As the glucose concentrations present in media were increased,

TDM production decreased, whereas the amount of TMM remained constant (Fig. 1*A*, *lanes 2–6*). Also, an increase in a discrete, unknown lipid species with a retardation factor (R_f) slightly greater than that of TDM was noted (Fig. 1*A*, *lanes 3–6*, indicated with an *arrow*). To determine the molecular identity of the unknown lipid, it was purified and subjected to TLC and MS analyses. The purified lipid was resolved as doublet bands on a TLC plate developed with a solvent system of C/M (9:1, v/v) (Fig. 1*B*). MALDI-TOF MS analysis revealed that the mass numbers of given ions were matched with those of sodium adducts of hexose monomycolate (Fig. 1*C*). Within the limits of error of the method of detection, the masses matched both in terms of the expected *m/z* of the dominant ions, the range of mass variation expected of individual molecular species of mycolate derivatives, and the absolute mass differences among the major ions, which can be accounted for by differences in carbon chain length and substitution of R groups (14). For example, *m/z* 1452.4 corresponds to the expected mass of sodium adduct of hexose monomycolate with C_{85} fatty acid and a wax ester-type R group on the meromycolate chain (Fig. 1*C*). GC-MS analysis of an alditol acetate derivative of the sugar moiety derived from the purified lipid identified glucose as the hexose group attached to mycolates (Fig. 1*D*). The doublet bands observed on a TLC plate were thus likely to represent two stereoisomers of mycolates as described previously (5, 15). Finally, the production of GMM in response to added glucose is expected based on the ability of mycobacteria to couple abundant hexose sugars at mycolyl esters (5). These results detected a reciprocal production of TDM and GMM by MAC in response to exogenous glucose without apparent alterations in the steady state levels of TMM. This experiment, carried out in live bacteria, raised the possibility that mycolyltransferases might compete for carbohydrate substrates.

Ag85 Utilized Glucose for GMM Biosynthesis—Mycobacteria-derived mycolyltransferases, known also as Ag85, catalyze the final step of TDM biosynthesis, using TMM as a substrate. Current models of the Ag85-catalyzed reaction predicted that two molecules of TMM are captured in the two substrate-binding pockets of the enzyme, and the mycolyl acyl group of the TMM substrate bound in one substrate-binding pocket (donor site) is transferred to the other TMM substrate bound in the other pocket (acceptor site), resulting in generation of one molecule of TDM and one molecule of trehalose (Fig. 2*A*) (2, 16). Although GMM can be an abundant structure in the cell wall and functions to activate T cells and form granulomas, its mechanism of synthesis was unknown. We hypothesized that GMM biosynthesis could be catalyzed by Ag85 if glucose, instead of TMM, occupied the acceptor site (Fig. 2*B*). To address this possibility, we made recombinant Ag85A enzyme from the *M. avium* strain (serovar 4), and we performed *in vitro* enzymatic reaction experiments. To accomplish this, we first carried out PCR from the genome of the MAC strain as a template, and isolated the Ag85A gene that encoded the mature protein lacking the signal sequence. DNA sequencing of the isolated gene revealed that three nucleotides were altered as compared with the previously reported Ag85A gene derived from *M. avium* serovar 1 strain (17), but the deduced amino acid sequences were identical in both strains. We then constructed an expression plasmid in which the initiation codon was placed at the 5′-end and the sequence encoding a His tag was attached in frame at the 3′-end of the isolated Ag85A gene. The His-tagged enzyme was expressed in *E. coli* and affinity-purified by Ni^{2+}-charged resin column chromatography. The purified material was resolved as a single band with an apparent molecular mass of ~33 kDa on a Coomassie-stained SDS-polyacrylamide gel, consistent with its being the Ag85A protein (Fig. 3*A*). Incubation of TMM *in vitro* in the presence of this

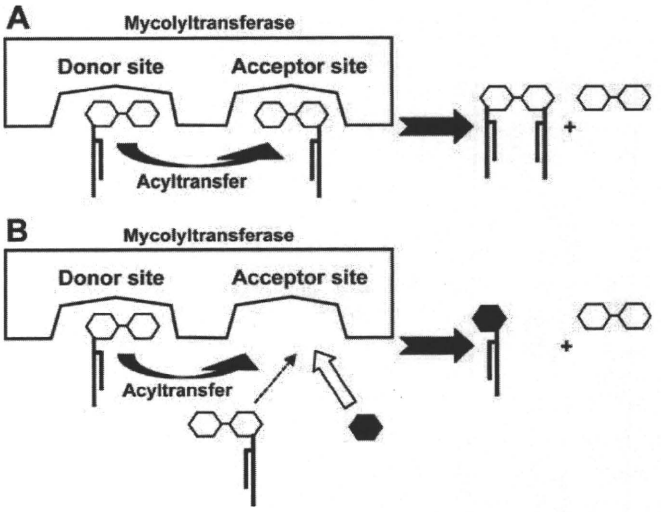

FIGURE 2. **Proposed scheme for TDM (*A*) and GMM (*B*) production catalyzed by mycolyltransferase.** In *model A*, both the donor site and the acceptor site of the enzyme interact with TMM, resulting in TDM formation. In *model B*, a glucose substrate competes against a TMM substrate for access to the acceptor site. When glucose is readily available, glucose rather than TMM preferentially gain access to the site, resulting in production of GMM.

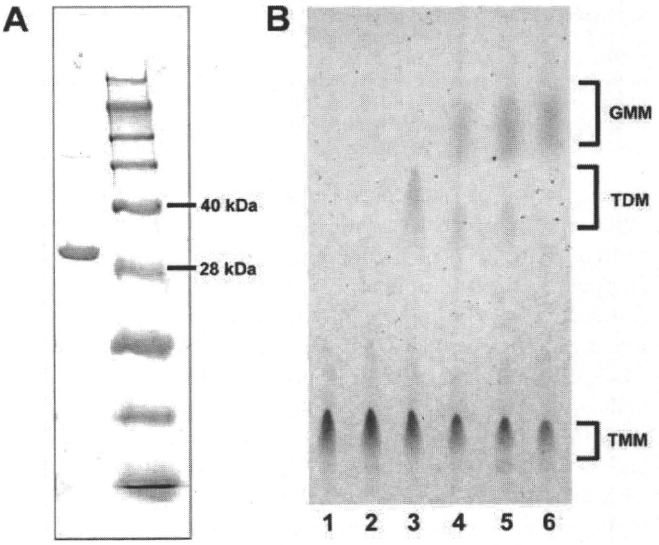

FIGURE 3. **TDM-GMM exchange mediated by recombinant Ag85A.** *A*, purified MAC Ag85A (*left lane*) and a size marker (*right lane*) were resolved on a Coomassie-stained SDS-polyacrylamide gel. Positions for the 40- and 28-kDa marker proteins are indicated. *B*, enzymatic reactions were performed at 37 °C at conditions indicated below, and the lipids were extracted from the reaction mixtures, followed by analysis on a TLC plate. *Lane 1*, Ag85A and TMM with 5% glucose (w/v), 0 h of incubation; *lane 2*, heat-inactivated (100 °C, 3 min) Ag85A and TMM with 5% glucose (w/v), 1 h of incubation; *lanes 3–6*, Ag85A and TMM either with 0.2% (w/v) glucose (*lane 4*), 1% glucose (w/v) (*lane 5*), and 5% (w/v) glucose (*lane 6*) or without glucose (*lane 3*), 1 h of incubation.

enzyme preparation resulted in generation of TDM (Fig. 3*B*, *lane 3*), confirming the mycolyltransferase activity exerted by the recombinant protein. Strikingly, addition of glucose to this reaction condition resulted in decreased TDM production in a dose-dependent manner, which was associated with an increase in GMM (Fig. 3*B*, *lanes 3–6*). GMM synthesis was completely abrogated when heat-inactivated enzyme was used (Fig. 3*B*, *lane 2*). This further confirmed that GMM was produced enzymatically by the mycolyltransferase activity of Ag85A but not as a result of nonenzymatic hydrolysis. These results indicate that Ag85A mediates synthesis of GMM. In this molecular model, we propose that TMM and glucose compete for access to the acceptor site of the Ag85A, and the enzyme preferentially catalyzes biosynthesis of GMM, rather than TDM, when glucose is readily available (Fig. 2*B*). The substrate selection by the mycolyltransferase would likely provide a molecular basis for the glucose-dependent TDM-GMM exchange detected in cultured MAC.

GMM Production Occurs at a Physiological Glucose Concentration—The observations made above have established an enzymatic pathway for GMM production in live mycobacteria that are grown in the presence of high levels of exogenous glucose. However, it remains to be addressed whether mycobacteria can produce GMM under physiological concentrations of glucose present in mammalian hosts, which is maintained at ~100 mg/dl (0.1% w/v). To address this issue, we measured GMM production by mycobacteria cultured in liquid media with a glucose concentration comparable with that in the host. The MAC culture was started in the presence of either 0.01 or 0.1% glucose, and every 24 h, the culture media were replaced with fresh media to maintain the glucose concentrations at constant levels. After 5 days of culture, the bacteria were harvested, and the total lipids were extracted. Subsequently, methanol-insoluble lipids were isolated from these total lipids, followed by separation on TLC plates (Fig. 4*A*). Although TDM production was readily detected in both cultures, GMM production was detected only in the presence of 0.1% glucose (Fig. 4*A*, *lane 2*) but not in the presence of 0.01% glucose (*lane 1*). This was also confirmed by T cell-based assays (Fig. 4*B*) in which Jurkat T cells expressing specific TCRs recognizing GMM in the context of CD1b molecules were used. Incubation of the T cells with CD1b-expressing cells (C1R/CD1b) in the presence of the total lipids from the 0.1% glucose-containing culture resulted in dose-dependent IL-2 production by the T cells, demonstrating high levels of antigenicity when growing at physiological glucose concentrations (Fig. 4*B*, *upper panel*). The specific response was not observed when CD1b-negative cells (C1R/mock) were used as antigen-presenting cells, supporting that the response was CD1b-restricted.

We then addressed how quickly induction of GMM production occurred after exposure to 0.1% glucose. MAC was cultured either in liquid media containing 0.01% (Fig. 5*A*) or 0.1% (*B*) or in human serum (*C*), and the bacteria were harvested at 2, 4, 8, 18, and 24 h. GMM production was observed as early as 8 h after the start of the culture both in 0.1% glucose-containing media and in human serum but not in media containing 0.01% glucose. These observations suggest that GMM production can occur quickly after exposure to high levels of glucose presumably as a result of competitive substrate selection by preexisting mycolyltransferases.

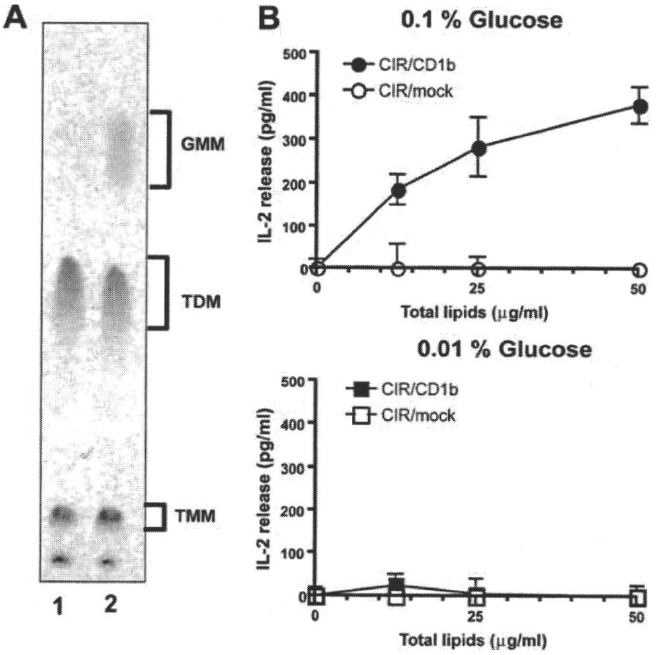

FIGURE 4. **GMM production by mycobacteria cultured at a physiological glucose concentration.** *A*, MAC was cultured in liquid media containing either 0.01 or 0.1% glucose, and the culture media were replaced with fresh media every day to maintain the glucose concentrations. After 5 days, the bacteria were harvested, and the total lipids were extracted. The methanol-insoluble fraction was then obtained from 100 μg of each total lipid preparation and analyzed by TLC. *B*, GMM-specific, CD1b-restricted TCR-expressing Jurkat T cells were cocultured with either C1R/CD1b or C1R/mock in the presence of different concentrations of the total lipids derived from the 0.1% glucose-containing (*upper panel*) and the 0.01% glucose-containing (*lower panel*) cultures. The T cell response was assessed by measuring IL-2 released into the media.

GMM Production Occurs in Mycobacteria-infected Tissues—A previous study detected GMM comigrating lipids can be derived from *Mycobacterium leprae*, raising the possibility that GMM is produced by mycobacteria in tissues (5). However, the chemical structures of such candidate glycosyl mycolates could not be directly determined, and it remained unknown whether *M. tuberculosis* produces GMM during infection. Therefore, we infected CH3 mice with *M. tuberculosis* Erdman strain and isolated mycobacteria directly from the lungs after ~3 weeks of infection. Bacteria were enriched from lung preparations by centrifugation and treatment with weak base to disperse lung tissue. The resulting preparations contained predominantly mycobacterial lipids when analyzed by LC-MS (data not shown). By comparing total *M. tuberculosis* lipids from lung with an *M. fallax* GMM standard in LC-MS experiments, we analyzed the *in vivo* derived lipids that nearly copurified with the GMM standard. Mass measurements with an Accurate Mass QTOF capable of mass resolution of 10 ppm detected an ion at 1317.2577 in lung-derived lipids (Fig. 6*A*). Both the absolute *m/z* and the isotope ratios matched the predicted masses of an ammonium adduct of a GMM carrying a C_{78} α-mycolic acid within expected error (C_{84}, $H_{162}O_8$, C_{78} GMM, expected *m/z* 1317.2613). Further supporting the identification of this ion as GMM, mycolic acid derivatives are characteristically synthe-